

Precision Observations of Galaxy Clusters through Broadband Spectroscopy of the Sunyaev-Zeldovich Effect

Luca Lamagna (on behalf of P. de Bernardis)

Physics Department

Sapienza-University of Rome



Outline

- **C**luster science and SZ effect
 - Advantage of multi-frequency observations
 - Spectrometry of the SZE
- **O**limpo DFTS
 - Instrument rationale
 - Subsystems review
 - Projected performance
- **F**inal Remarks

What are galaxy clusters?

«Galaxy clusters are significant concentrations of galaxies.»



Basically true, but...

What are galaxy clusters?

«Galaxy clusters are significant concentrations of galaxies.»



Basically true, but...fairly naive.

What *truly* are galaxy clusters?

- «Galaxy Clusters are the cosmic structures on the high-mass tail of the halo mass function»
- Large structures (few Mpc) with a fair representation of the cosmic mass budget:
 - ~ 2% mass in galaxies (tens to thousands depending on richness)
 - ~ 13% in the hot ($10^7\div 10^8\text{K}$), ionized intra-cluster plasma (i.e. baryon assembly into galaxies is quite inefficient)
 - ~ 85% dark matter (historical argument by F. Zwicky)Typical masses in excess of $10^{14} M_{\odot}$
- Routine observations of clusters today are performed in a variety of spectral windows:
 - Optical, IR (σ_v, N_{gal})
 - Optical (lensing mass)
 - X-rays (L_x, T_x)
 - Mm/submm (Compton Y)
 - Radio (halos, relics...)
 - ...

Clusters: the crossroad of astrophysics and cosmology?

- Measuring distances using clusters as standard rulers
- Growth of cosmic structure from cluster number counts
- Calibration of the SZ flux vs total mass scaling relation
- Using the gas mass fraction in clusters to measure the cosmic baryon density
- Measuring the large-scale velocity fields in the universe from kinematic SZ Effect
- Constraints from power spectrum
- Constraints on $T_{\text{cmb}}(z)$

Problem: at the Mpc scales, structure assembly and evolution cannot be predicted from pure gravity+cosmology alone.

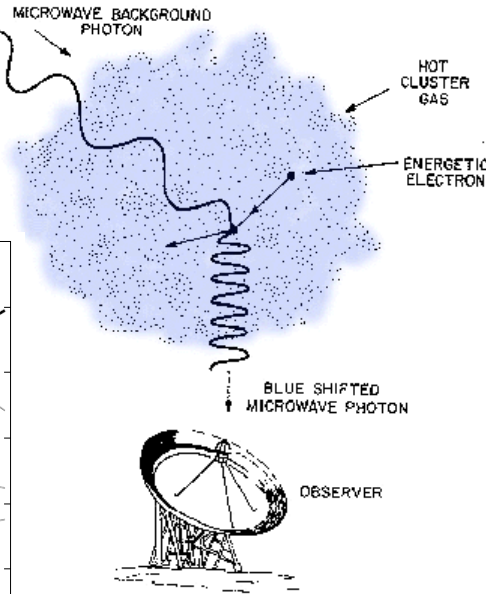
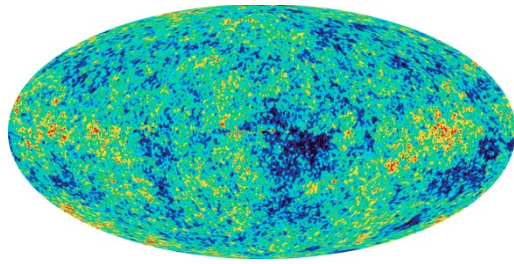
Q: Given this complication, can we still predict some general properties which bind the cluster population to the underlying cosmology?

A: Yes, if we understand the (baryon) physics in galaxy clusters.

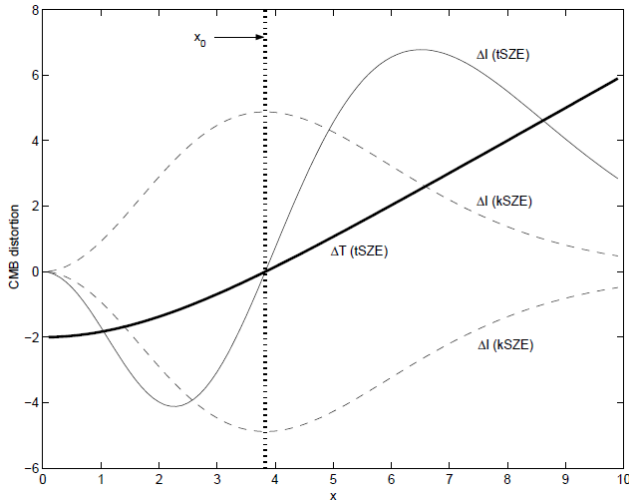
Baryons in galaxy clusters

- Assembly into galaxies is inefficient
- Majority of baryonic mass in clusters is hot gas (ICM)
 - Temperature $T \sim 10^8$ K (~ 10 keV) (heated by gravitational potential)
 - Electron number density $n_e \sim 10^{-3}$ cm $^{-3}$
 - Mainly H, He, but with heavy elements (O, Fe, ..)
 - Mainly emits X-rays (but also radio and gamma rays), first observed by Uhuru back in the '70s
 - $L_x \sim 10^{45}$ erg/s, most luminous extended X-ray sources in Universe
 - Causes the Sunyaev-Zel'dovich effect (SZE) by inverse Compton scattering the background CMB photons

Clusters at CMB frequencies: the Sunyaev-Zel'dovich Effect



- Inverse Compton Scattering of CMB photons off the hot ICM electrons results in a net energy injection into the CMB photons.
- Photons are shifted to higher frequencies, providing a unique spectral signature of the CMB distortion at microwaves.
- «Holes in the microwave sky» at radio frequencies, hot spots above ~217 GHz.
- Redshift independent, first order in plasma density w.r.t. X-ray brightness: excellent tool to detect (and even discover) clusters at high z .
- Effect proportional to the integrated pressure of the ICM.



$$\Delta I = \frac{2k^3 T_{\text{CMB}}^3}{h^2 c^2} \frac{x^4 e^x}{(e^x - 1)^2} \sigma_T \int n_e dl [\theta f_1(x) - \beta + R(x, \theta, \beta)]$$

$$f_1(x) = x \coth\left(\frac{x}{2}\right) - 4$$

$$x = h\nu/kT_{\text{CMB}}$$

$$\theta = kT_e/mc^2$$

$$\beta = V_{\text{pec}}/c$$

Sunyaev & Zel'dovich, Comm. Astr. Sp. Phys 4, 173 (1972)

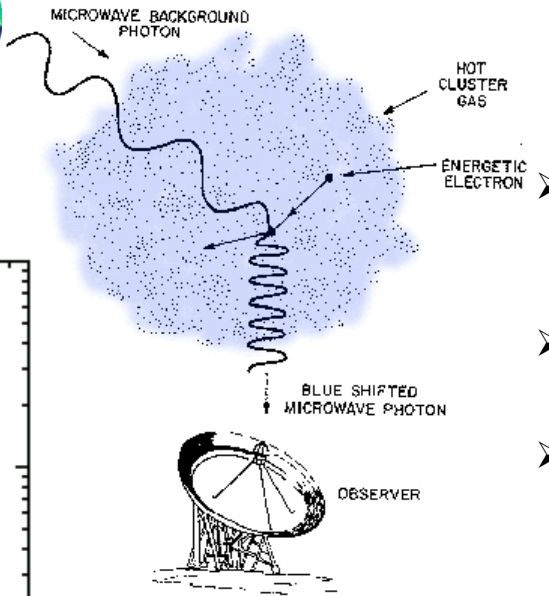
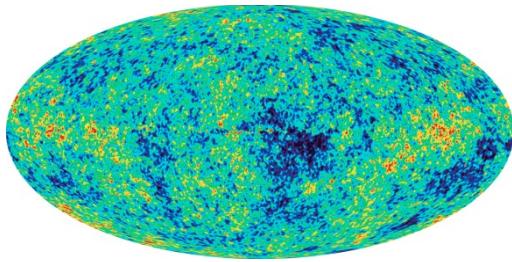
Reviews by:

Rephaeli, ARA&A 33, 541 (1995)

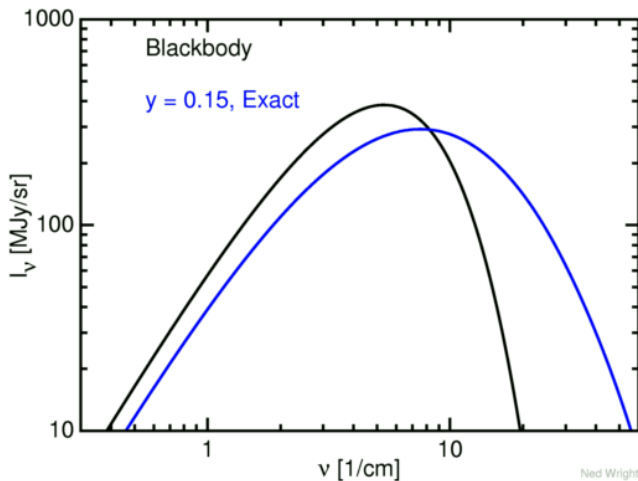
Birkinshaw, Phys. Rep. 310,97 (1999)

Carlstrom et al., ARA&A 40, 643 (2002)

Clusters at CMB frequencies: the Sunyaev-Zel'dovich Effect



- Inverse Compton Scattering of CMB photons off the hot ICM electrons results in a net energy injection into the CMB photons.
- Photons are shifted to higher frequencies, providing a unique spectral signature of the CMB distortion at microwaves.
- «Holes in the microwave sky» at radio frequencies, hot spots above ~217 GHz.
- Redshift independent, first order in plasma density w.r.t. X-ray brightness: excellent tool to detect (and even discover) clusters at high z .
- Effect proportional to the integrated pressure of the ICM.



$$\Delta I = \frac{2k^3 T_{\text{CMB}}^3}{h^2 c^2} \frac{x^4 e^x}{(e^x - 1)^2} \sigma_T \int n_e dl [\theta f_1(x) - \beta + R(x, \theta, \beta)]$$

$$f_1(x) = x \coth\left(\frac{x}{2}\right) - 4$$

$$x = h\nu/kT_{\text{CMB}}$$

$$\theta = kT_e/mc^2$$

$$\beta = V_{\text{pec}}/c$$

Sunyaev & Zel'dovich, Comm. Astr. Sp. Phys 4, 173 (1972)

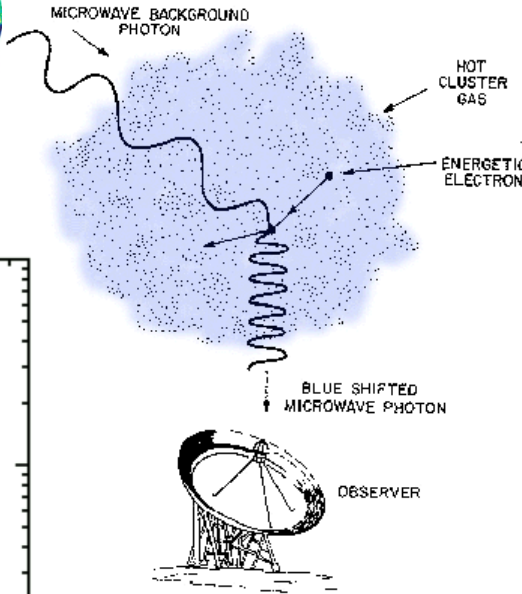
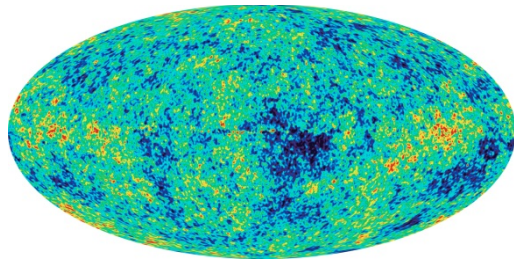
Reviews by:

Rephaeli, ARA&A 33, 541 (1995)

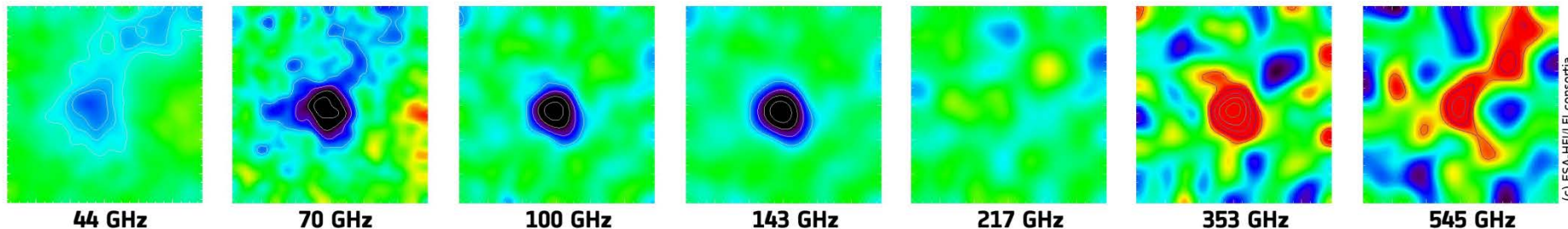
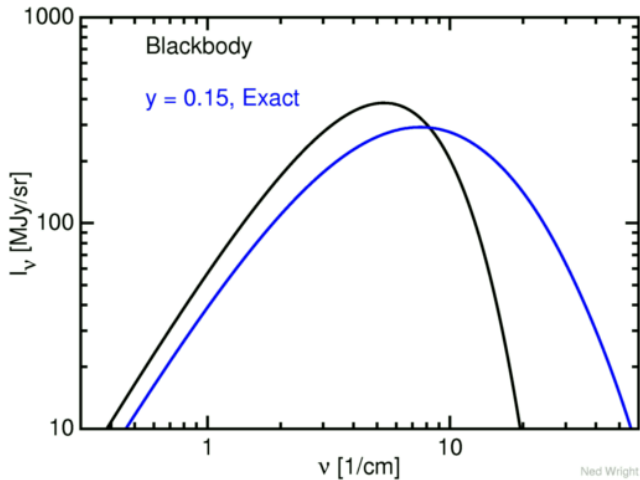
Birkinshaw, Phys. Rep. 310,97 (1999)

Carlstrom et al., ARA&A 40, 643 (2002)

Clusters at CMB frequencies: the Sunyaev-Zel'dovich Effect

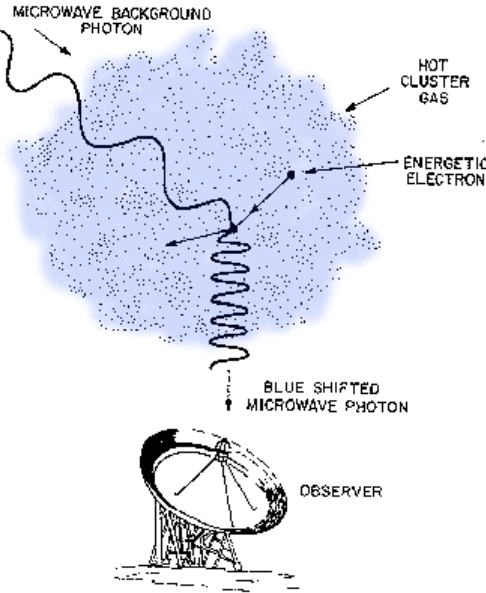
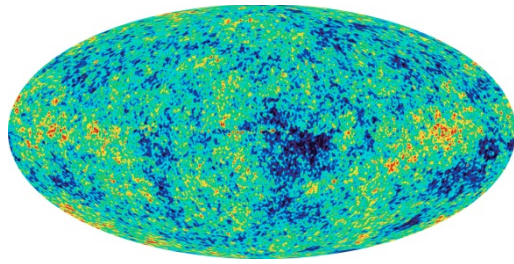


- Inverse Compton Scattering of CMB photons off the hot ICM electrons results in a net energy injection into the CMB photons.
- Photons are shifted to higher frequencies, providing a unique spectral signature of the CMB distortion at microwaves.
- «Holes in the microwave sky» at radio frequencies, hot spots above ~ 217 GHz.
- Redshift independent, first order in plasma density w.r.t. X-ray brightness: excellent tool to detect (and even discover) clusters at high z .
- Effect proportional to the integrated pressure of the ICM.

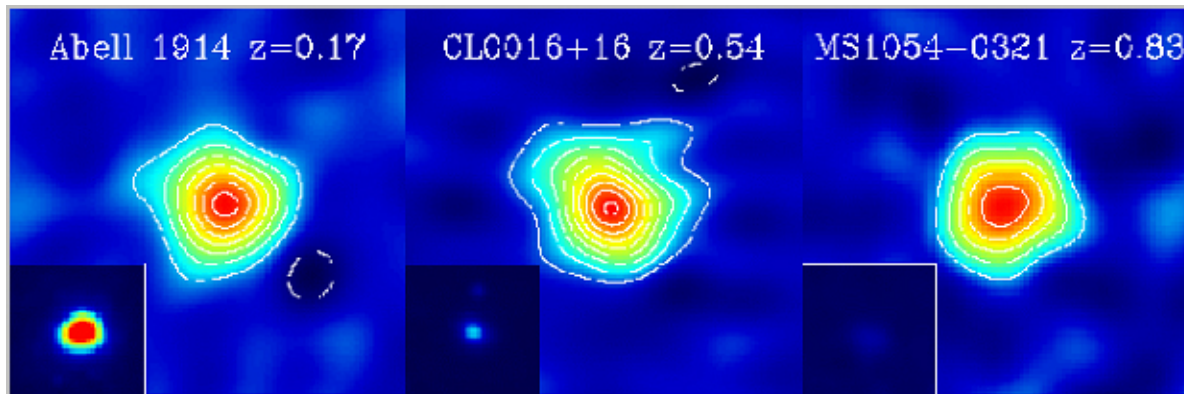
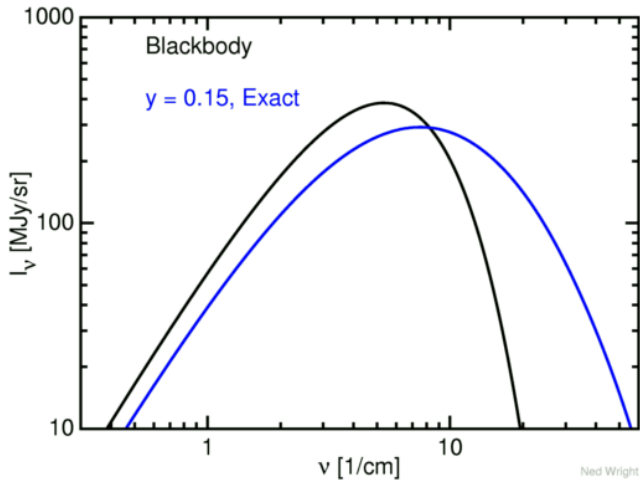


The spectral signature: Multifrequency view of Abell 2319 by Planck

Clusters at CMB frequencies: the Sunyaev-Zel'dovich Effect



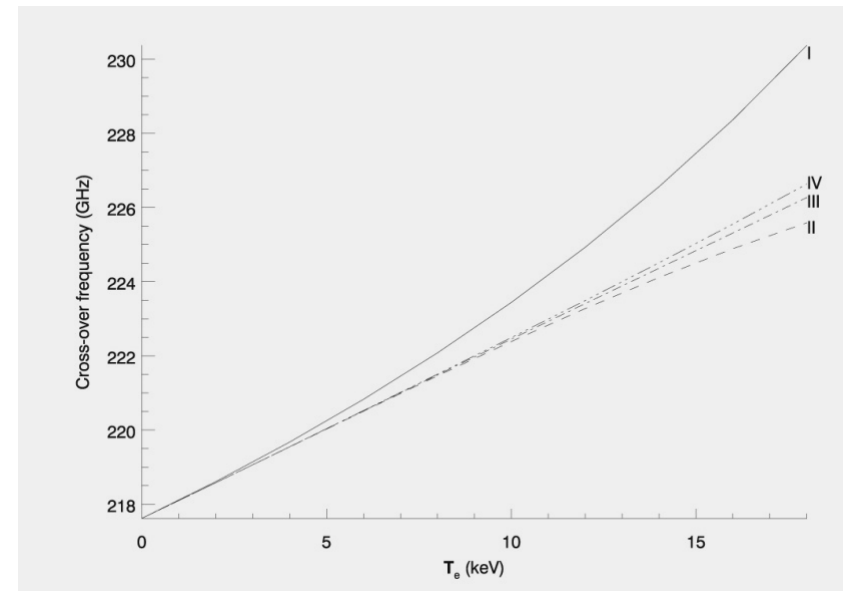
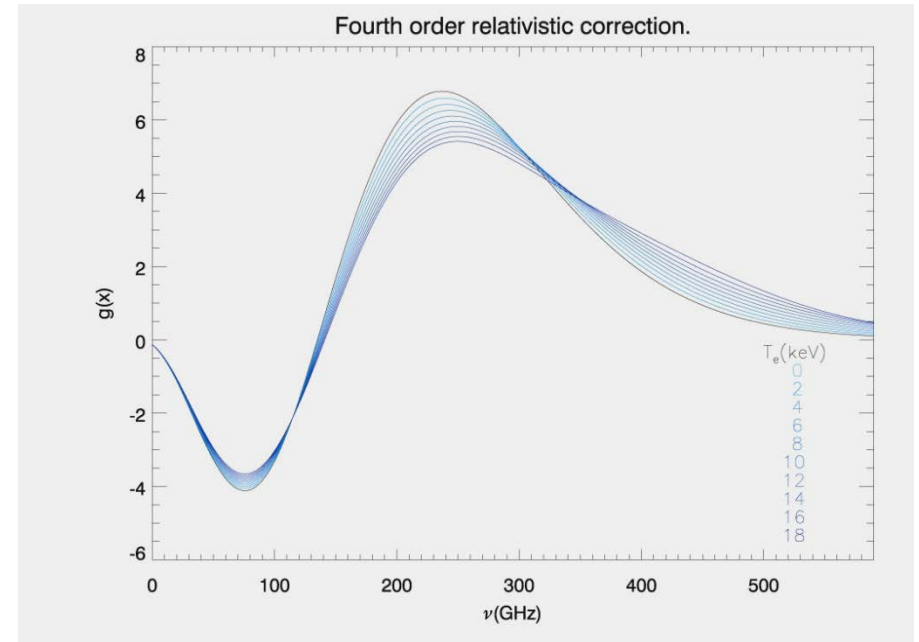
- Inverse Compton Scattering of CMB photons off the hot ICM electrons results in a net energy injection into the CMB photons.
- Photons are shifted to higher frequencies, providing a unique spectral signature of the CMB distortion at microwaves.
- «Holes in the microwave sky» at radio frequencies, hot spots above ~ 217 GHz.
- Redshift independent, first order in plasma density w.r.t. X-ray brightness: excellent tool to detect (and even discover) clusters at high z .
- Effect proportional to the integrated pressure of the ICM.



The redshift magic: OVRO/BIMA 30GHz maps with X-ray counterparts

Relativistic corrections

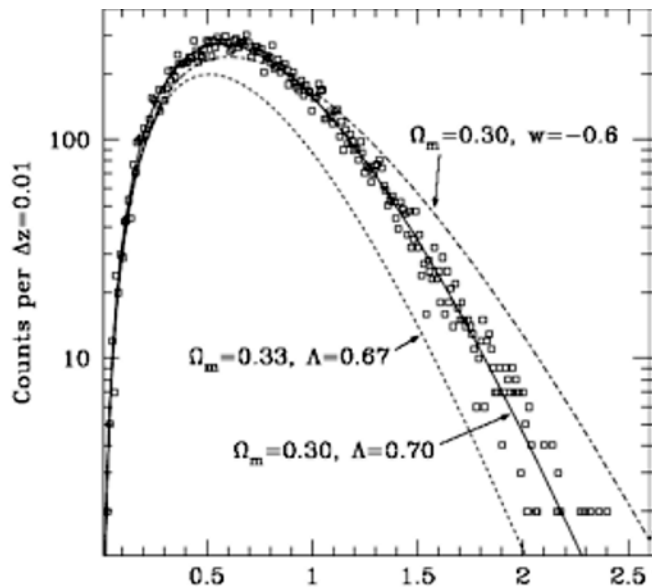
- Relativistic effects in the high velocity tail of the electron energy distribution do have an impact over the final comptonization effect, up to 10-15% in moderately hot ($kT_e > 8\text{keV}$) clusters.
- The relativistically correct crossover frequency is frequency dependent
- Observational consequences in cluster detection/selection and plasma characterization: need to clean signals and maps on a cluster-by-cluster basis, rather than statistically.
- Significant in blind surveys of unknown clusters.
- Measurements around the crossover and in the increment region are strongly sensitive to gas temperatures, providing a compelling probe of the baryon thermal history.



Cluster studies today

Cluster scaling relations & the quest for the perfect mass proxy

- How many clusters of mass M exist in a given cosmology at redshift z ?
- What is the probability that a cluster of mass M at redshift z will have temperature T_x (or some other observable)?



$$\frac{dN}{d\Omega dz} = \frac{dV}{d\Omega dz} \times \int_{M_{\min}}^{\infty} dM \frac{dn}{dM}$$

Comparison of mass-proxies + hydro sims can help identify which ones work best, but also provides insights on the relevant cluster physics.

How many «inferred» masses?

Hydrostatic (X, SZ):

$$\frac{dp_{\text{gas}}(r)}{dr} = -\rho_{\text{gas}}(r) \frac{G M_{\text{tot}}(<r)}{r^2} = \frac{k_B}{\mu m_p} \frac{d[\rho_{\text{gas}}(r) T_X(r)]}{dr}$$

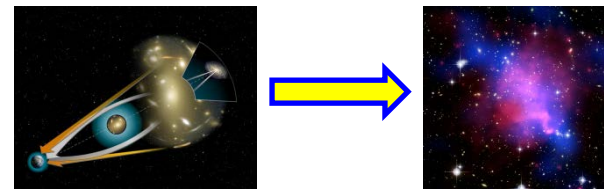
$$M_{\text{tot}}(<r) = -\frac{k_B T(r) r}{G \mu m_p} \left(\frac{d \ln \rho_{\text{gas}}}{d \ln r} + \frac{d \ln T}{d \ln r} \right)$$

$\mu \sim 0.6$: mean molecular weight; m_p : proton mass

Dynamical (opt):

$$M(r) = -\frac{r \sigma_r^2(r)}{G} \left[\frac{d \ln \sigma_r^2}{d \ln r} + \frac{d \ln \nu}{d \ln r} + 2\beta \right]$$

Lensing (opt):



Proxies: L_X , T_X , Y_X , Y_{SZ} , N_{200} , other?

$$Y_{S,\Delta} = \frac{\sigma_T}{m_e c^2} \frac{\mu}{\mu_e} \left(\frac{\sqrt{\Delta} G H_0}{4} \right)^{2/3} E(z)^{2/3} f_{\text{gas},\Delta} M_{\text{tot},\Delta}^{5/3}$$



Cosmology with cluster counts/masses

$$\frac{dN}{d\Omega dz} = \frac{dV}{d\Omega dz} \times \int_{M_{\min}}^{\infty} dM \frac{dn}{dM}$$

Different models/parametrizations for the Mass Function:

$$\frac{dn_M}{d \ln \sigma^{-1}} = \sqrt{\frac{2}{\pi}} \frac{\Omega_M \rho_{cr0}}{M} \frac{\delta_c}{\sigma} \exp\left[-\frac{\delta_c^2}{2\sigma^2}\right]. \quad (\text{Press-Schechter, 1974})$$

$$\frac{dn_M}{d \ln \sigma^{-1}} = A_J \frac{\Omega_M \rho_{cr0}}{M} \exp[-|\ln \sigma^{-1} + B_J|^{\epsilon_J}] \quad (\text{Jenkins, 2001})$$

$$\frac{dn_M}{d \ln \sigma^{-1}} = A \frac{\Omega_M \rho_{cr0}}{M} \left[\left(\frac{\sigma}{b}\right)^{-a} + 1 \right] e^{-c/\sigma^2} \quad (\text{Tinker, 2008})$$

Where:

$$\sigma^2 \propto \int_0^{\infty} P(k) W^2(kR) k^2 dk$$

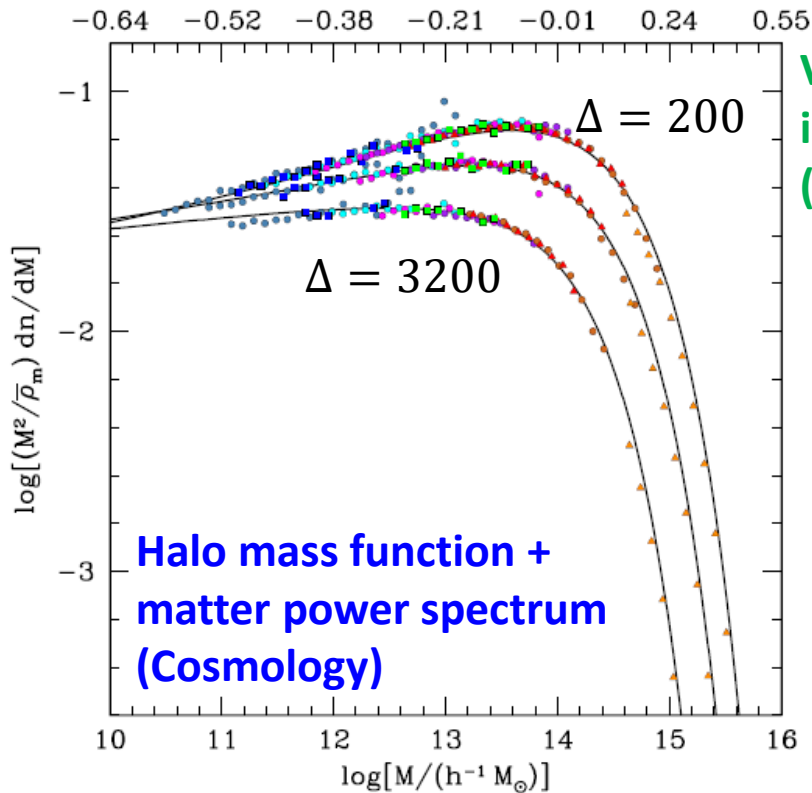
Variance on mass scale M
(constraints on σ_8 , Ω_m , Ω_Λ , w , ...)

Cosmology with cluster counts/masses

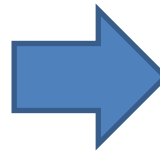
Cluster counts
(observations)

$$\frac{dN}{d\Omega dz} = \frac{dV}{d\Omega dz} \times \int_{M_{\min}}^{\infty} dM \frac{dn}{dM}$$

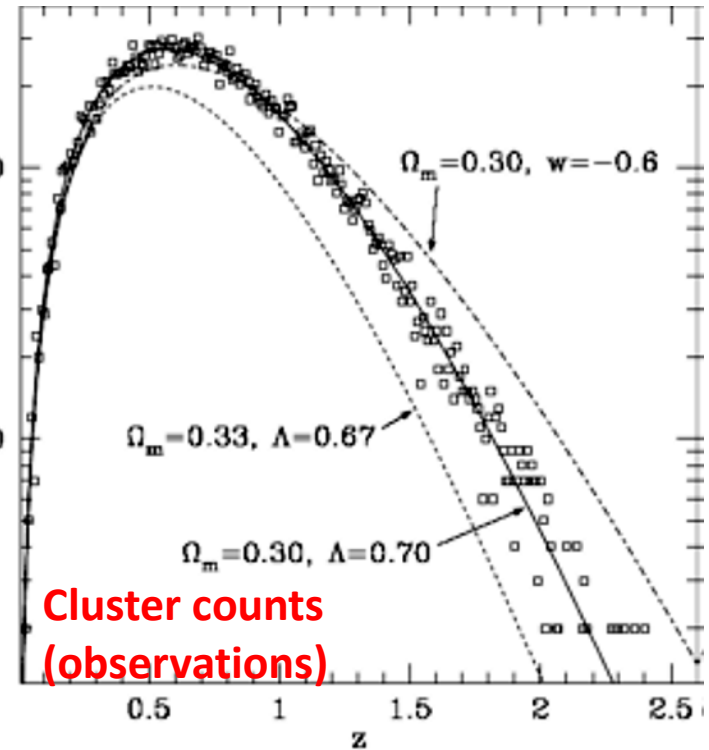
Halo mass function +
matter power spectrum
(Cosmology)



Volume
integration
(geometry)



Counts per $\Delta z = 0.01$



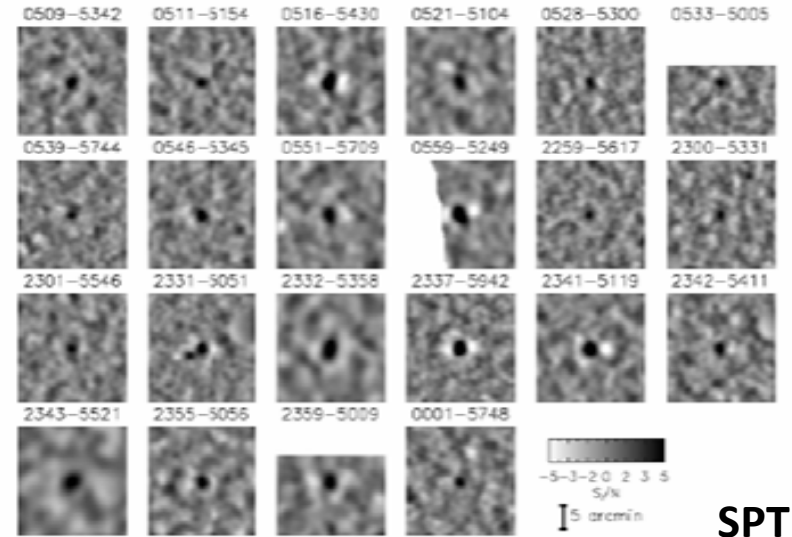
Cluster studies in the 2010s

Blind SZ detections & hi res SZ mapping



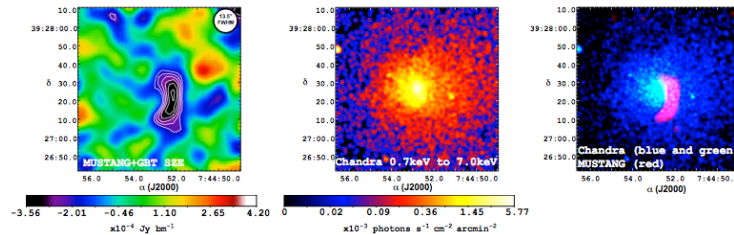
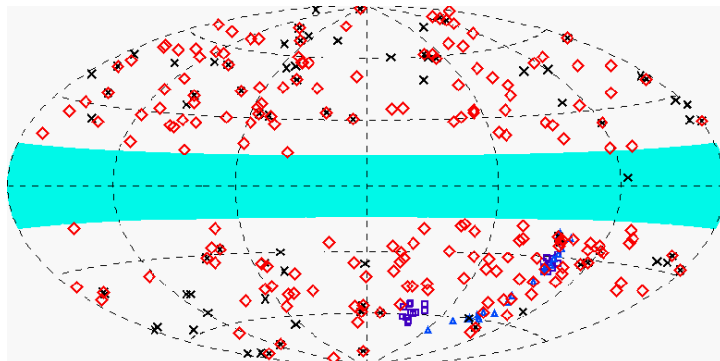
ACT

Marriage et al., ApJ 737, 71 (2011)



SPT

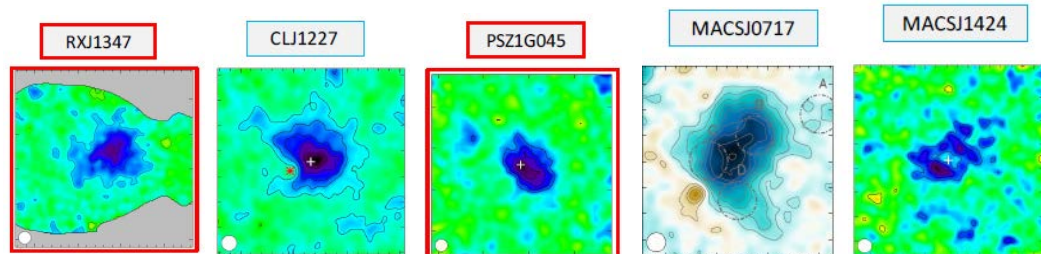
Vanderlinde et al., ApJ 722, 1180 (2010)



Mustang

Korngut et al., ApJ 734,10 (2011)

NIKA



well-known

high-z

Planck-discovered

disturbed cluster

point-source removal

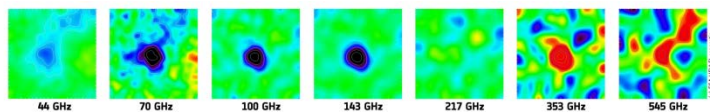
R. Adam et al., A&A 2014

R. Adam et al., A&A 2015

F. Ruppin et al., A&A 2017

R. Adam et al., A&A 2017

R. Adam et al., A&A 2016



Planck

(since early paper no. VIII)

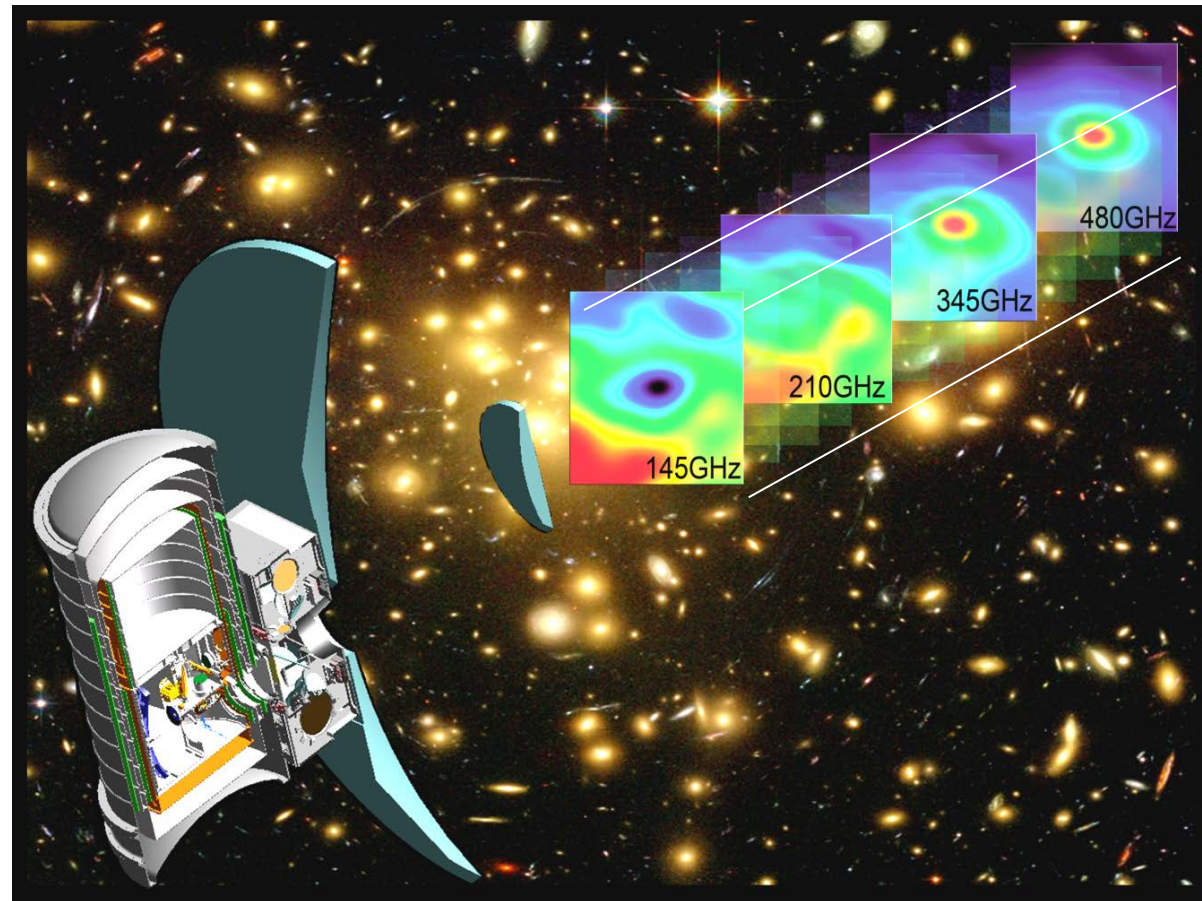
- Long Duration Balloon experiment for mm and sub-mm astronomy
- 2.6-m telescope with scanning capability by wobbling the primary mirror
- Multifrequency arrays (4) with kinetic inductance detectors

Two different observational modes in-flight:

- photometry
- spectrometry by DFTS

Main targets:

1. SZE on known clusters and blind survey
2. CMB power spectrum up to $l=2000$
3. FIRB



Team @ Uni. Sapienza: S. Masi (PI), P. de Bernardis, M. De Petris, F. Piacentini, E. Battistelli,
L. Lamagna, A. Coppolecchia, G. D'alessandro, A. Paiella, F. Columbro
F. Nati*, A. Schillaci*, R. Gualtieri*

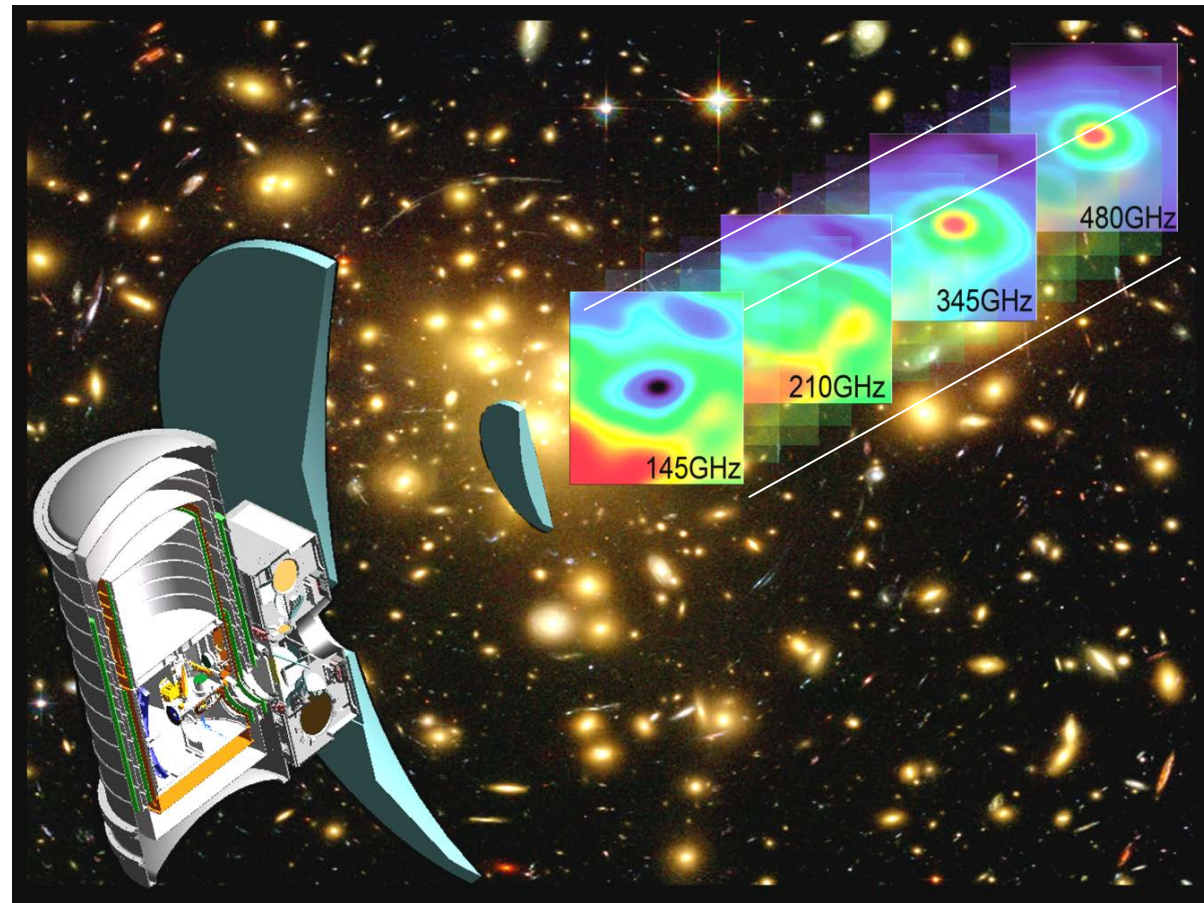
- Long Duration Balloon experiment for mm and sub-mm astronomy
- 2.6-m telescope with scanning capability by wobbling the primary mirror
- Multifrequency arrays (4) with kinetic inductance detectors

Two different observational modes in-flight:

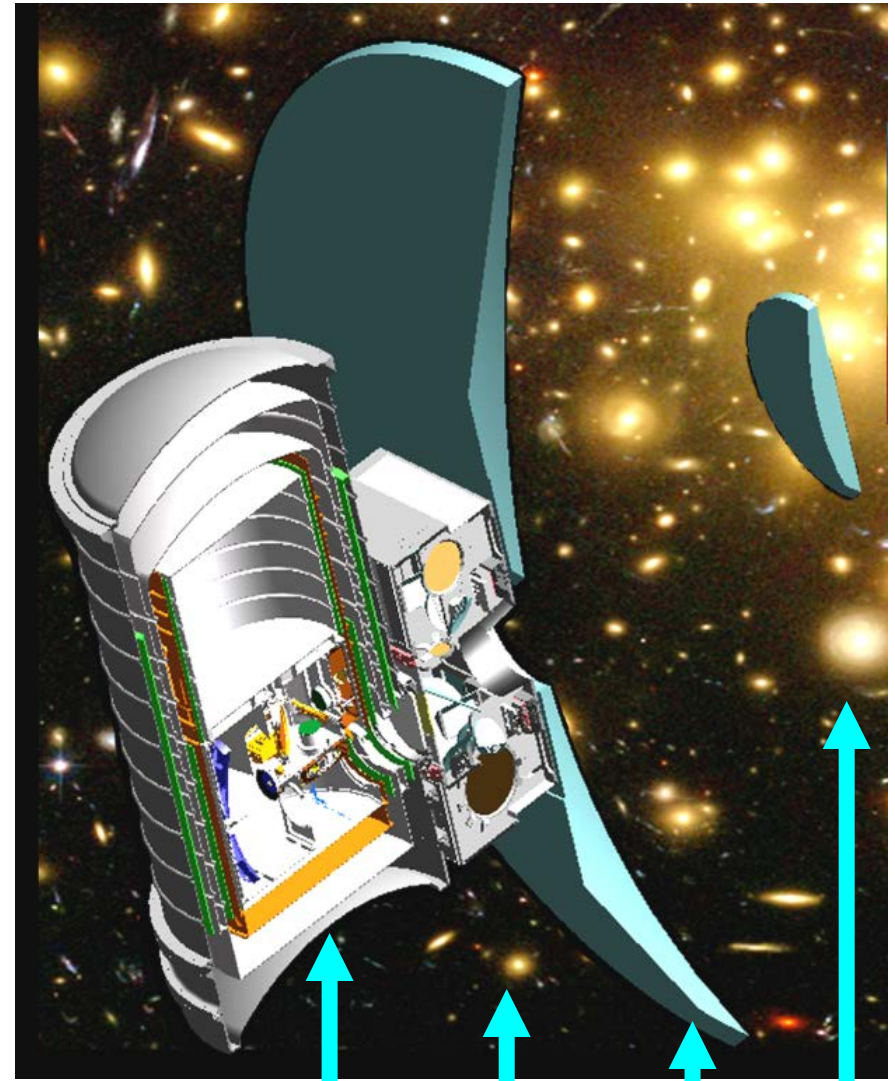
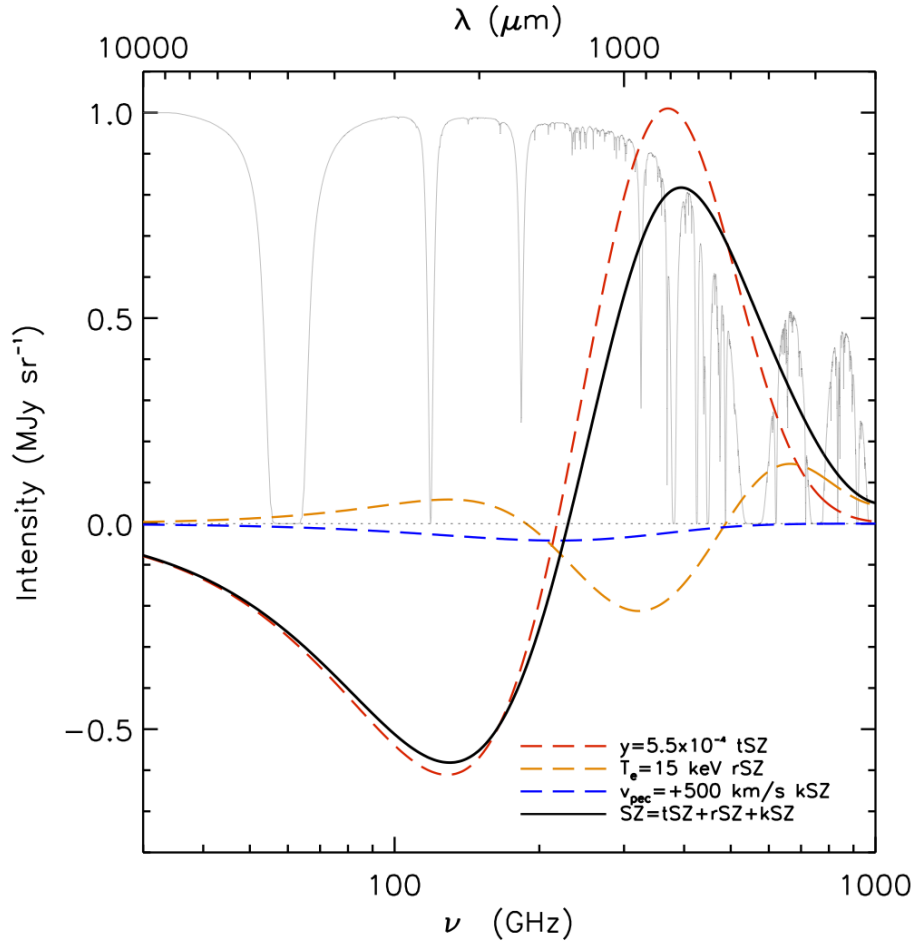
- photometry
- spectrometry by DFTS

Main targets:

1. SZE on known clusters and blind survey
2. CMB power spectrum up to $l=2000$
3. FIRB



OLIMPO – spectral coverage

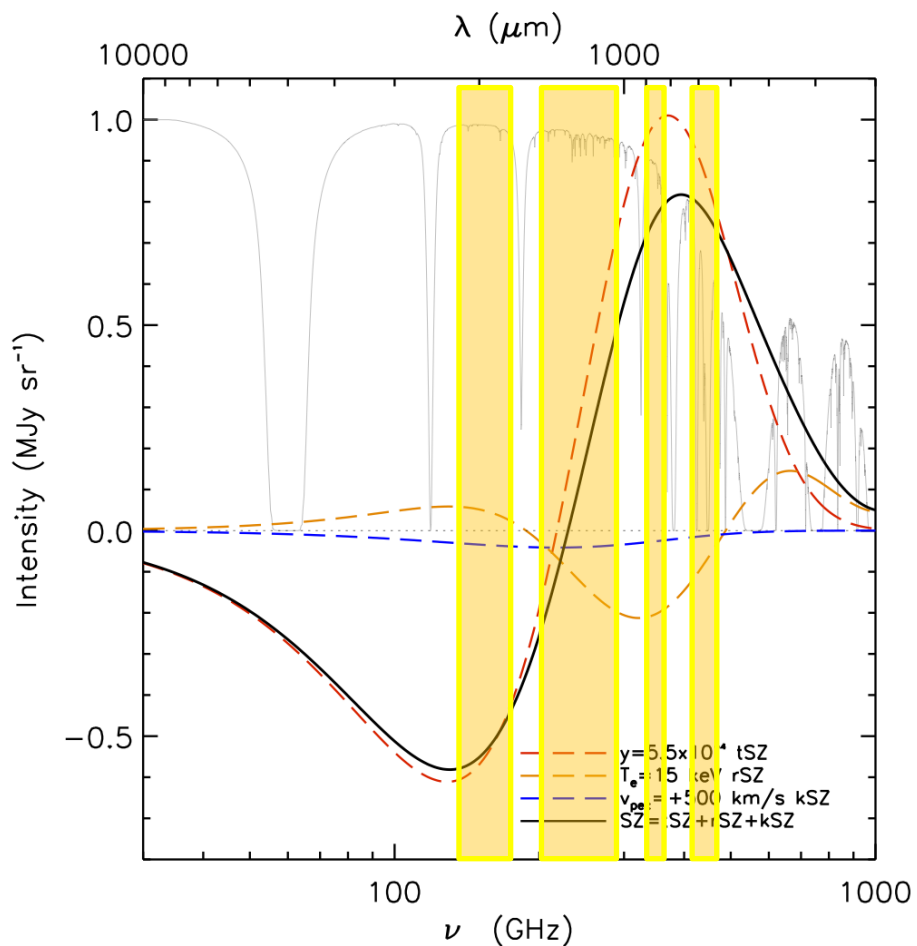


Cryostat
& det. arrays

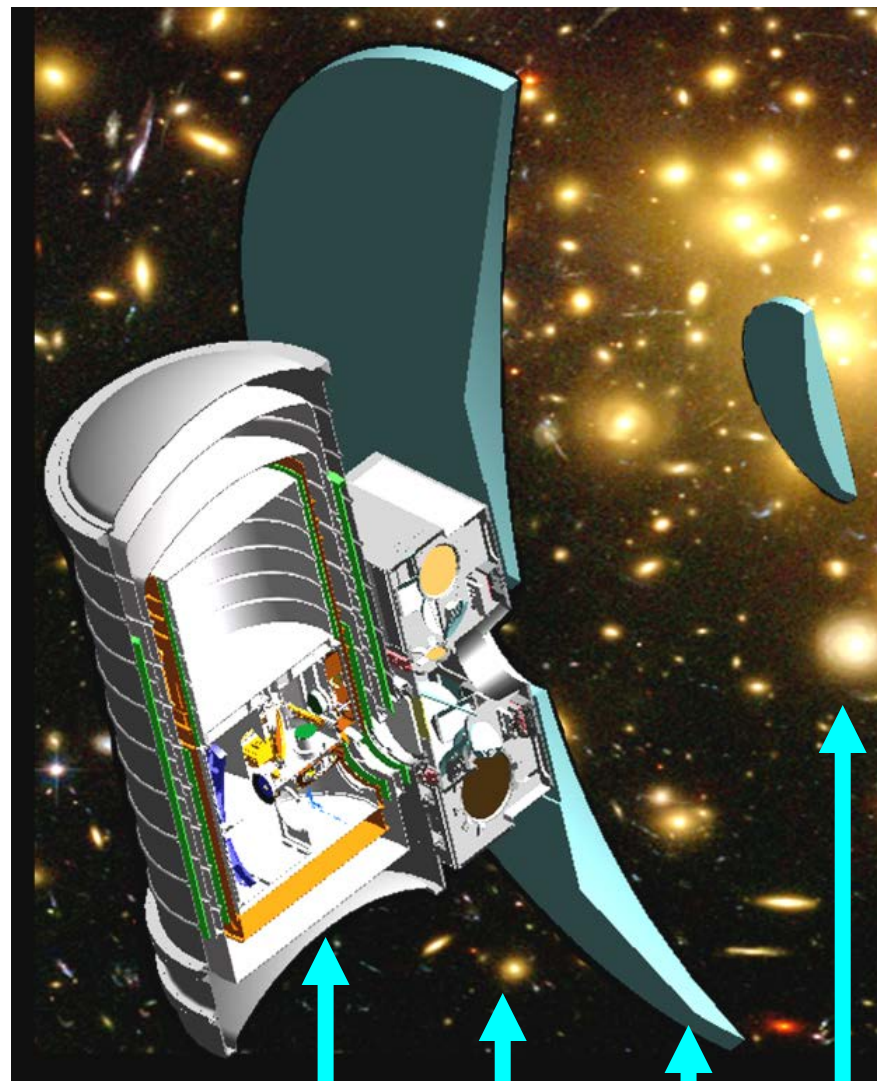
DFTS

telescope

OLIMPO – spectral coverage



# detectors	19	37	23	54
Photon bckg over band (pW)	9	19	17	60
Photon noise overband* ($10^{-18} W_{\text{rms}} / \sqrt{\text{Hz}}$)	200	140	170	200

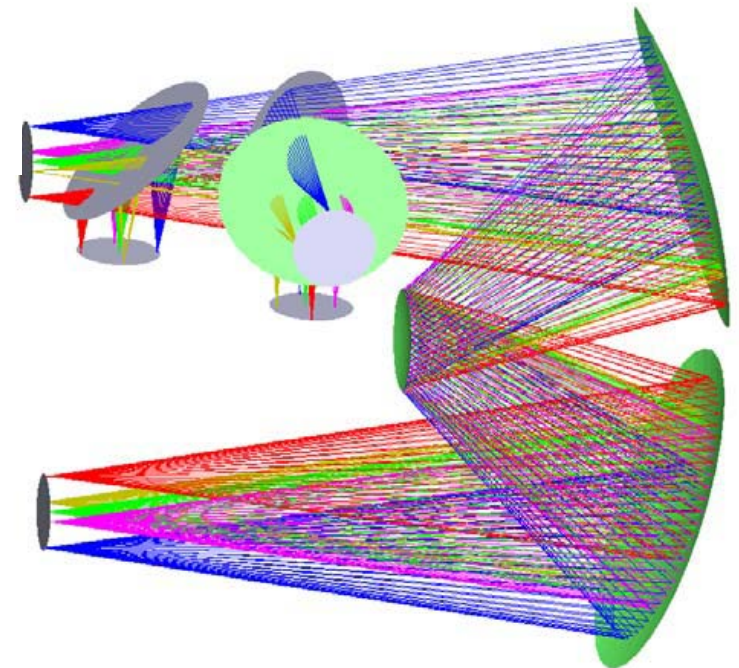
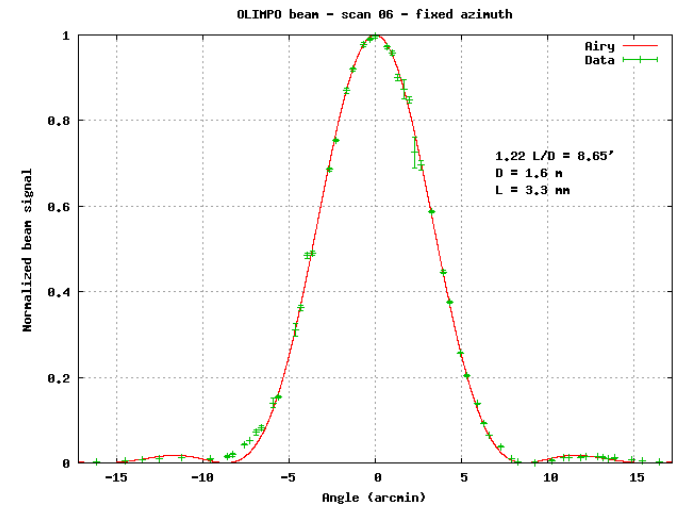
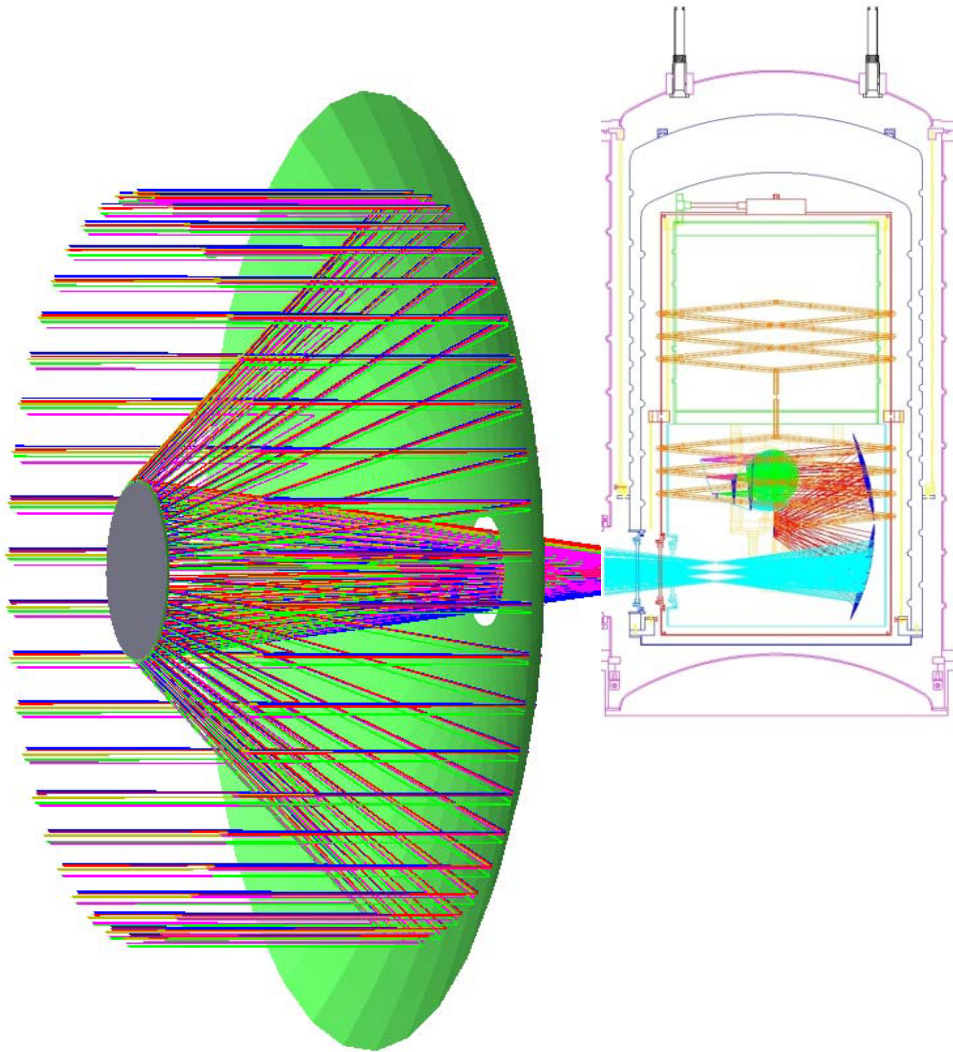


Cryostat
& det. arrays

DFTS

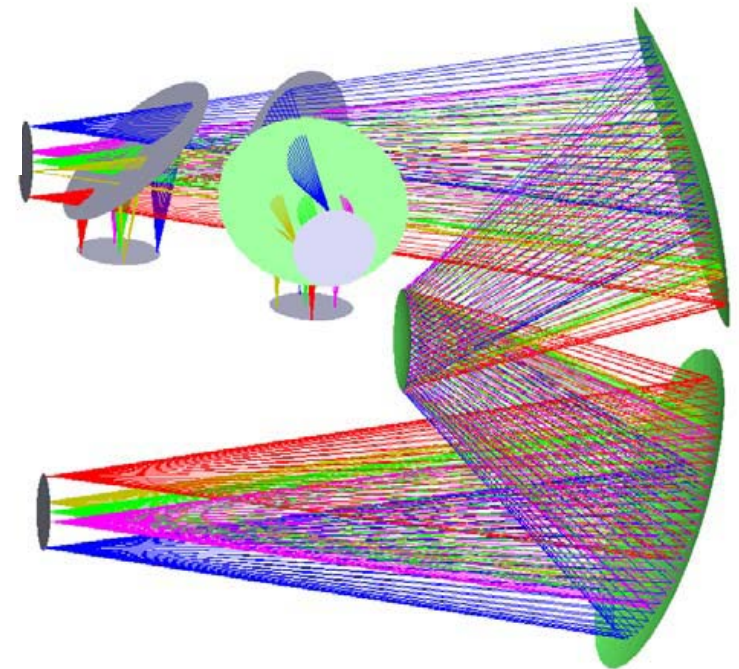
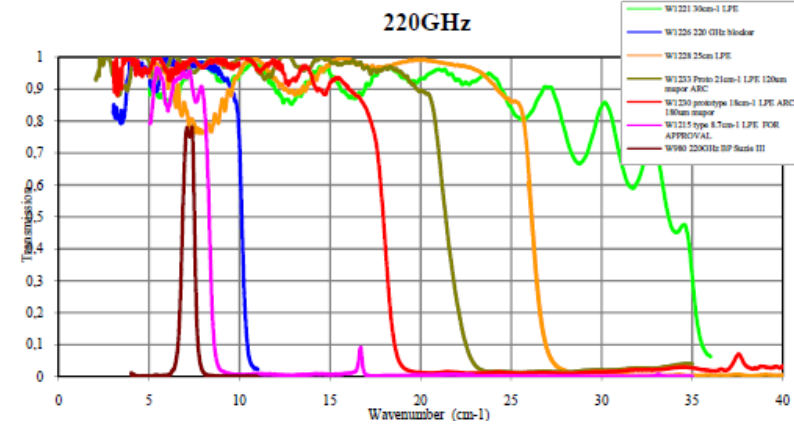
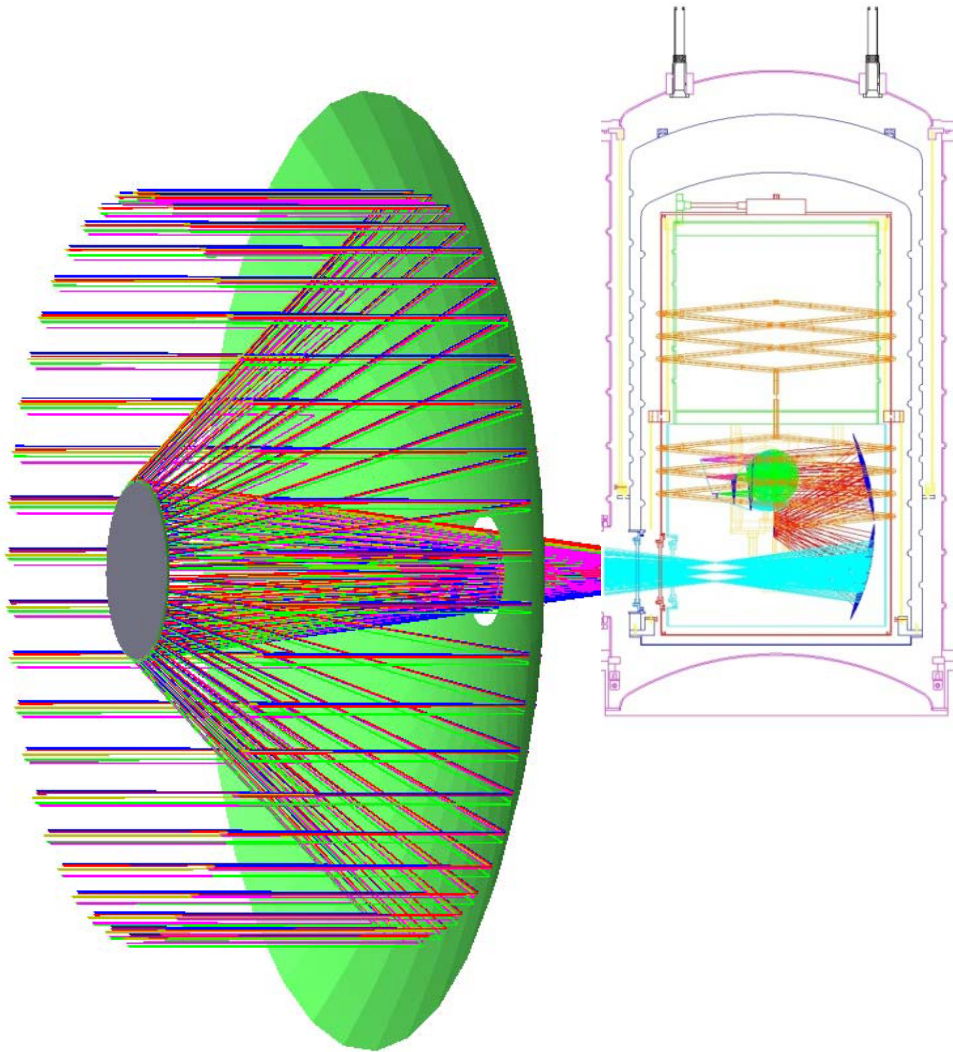
telescope

OLIMPO – telescope and cold optics



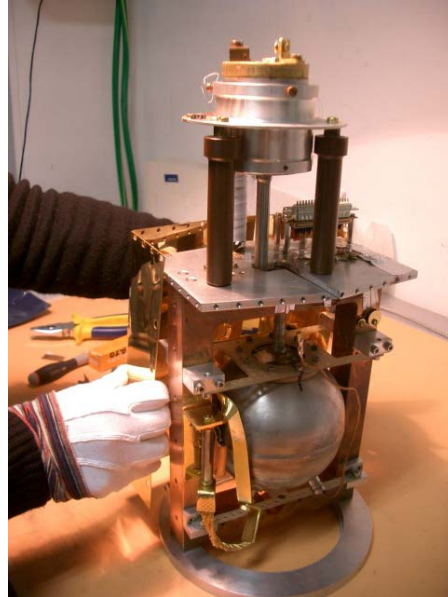
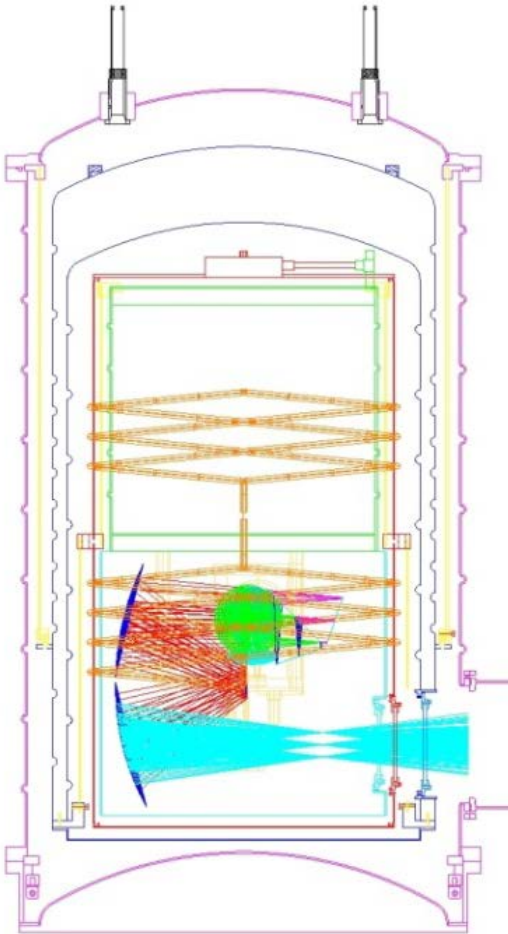
Modified Offner 1:1 design (M. De Petris+)

OLIMPO – telescope and cold optics



Modified Offner 1:1 design (M. De Petris+)

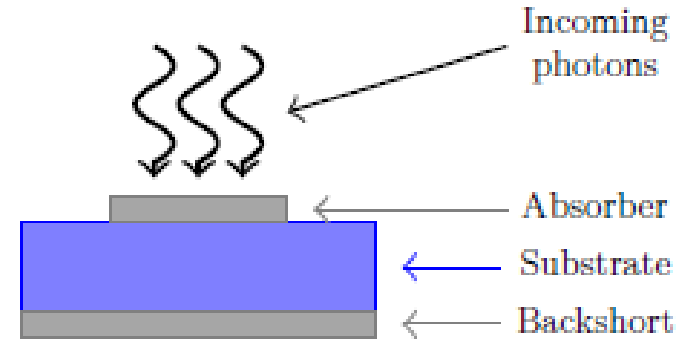
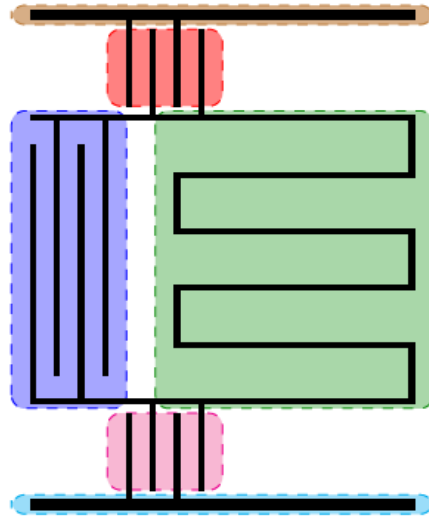
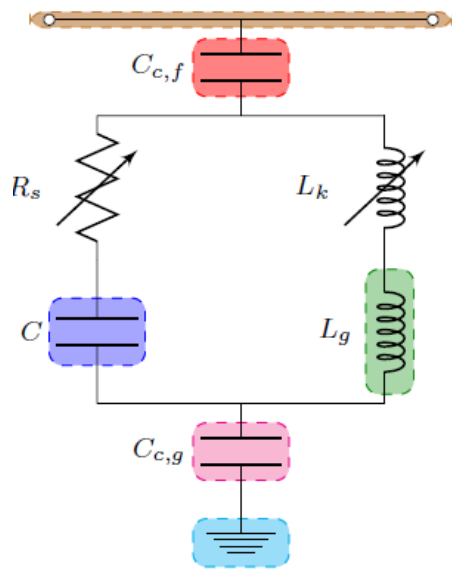
OLIMPO – wet cryostat & fridge



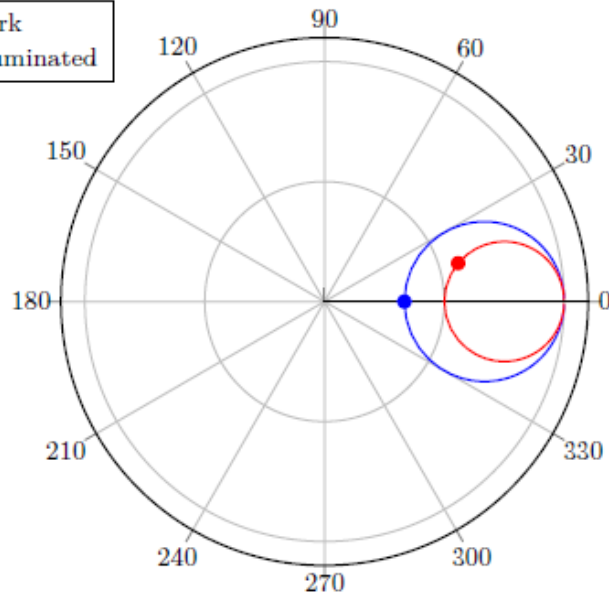
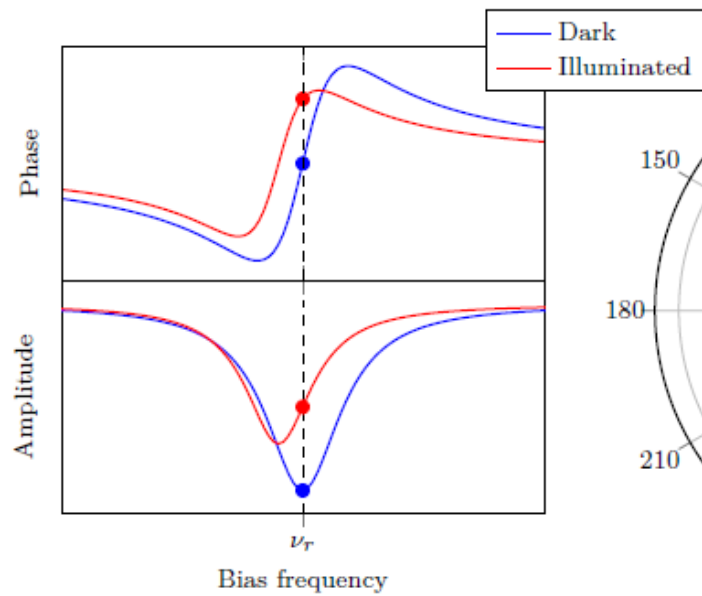
- Liquid N₂ + He Vapor Cooled Shield@20K + Liquid He@2K
- Single stage He³ sorption fridge
- Unmanned operation @ 300mK for 16days (suboptimal lab conditions) up to 45° tilt

Coppolecchia et al., in prep.

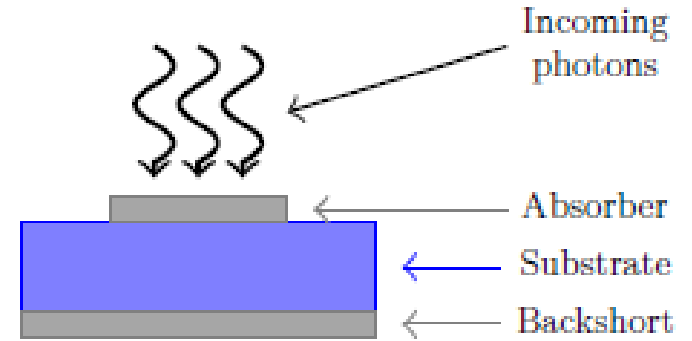
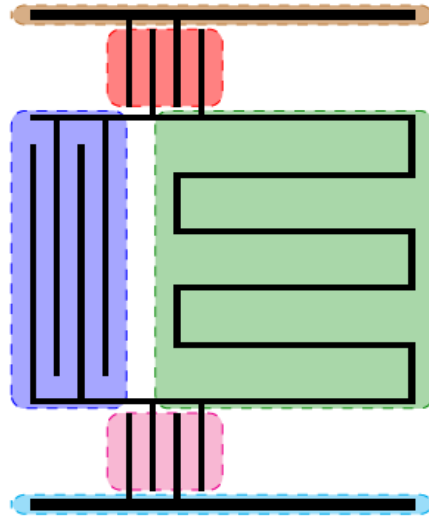
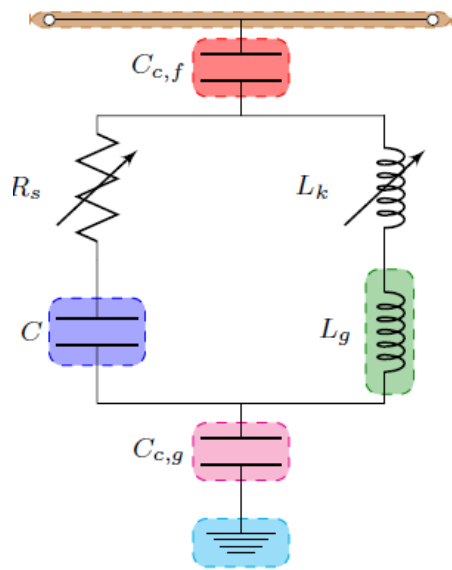
OLIMPO – KIDs



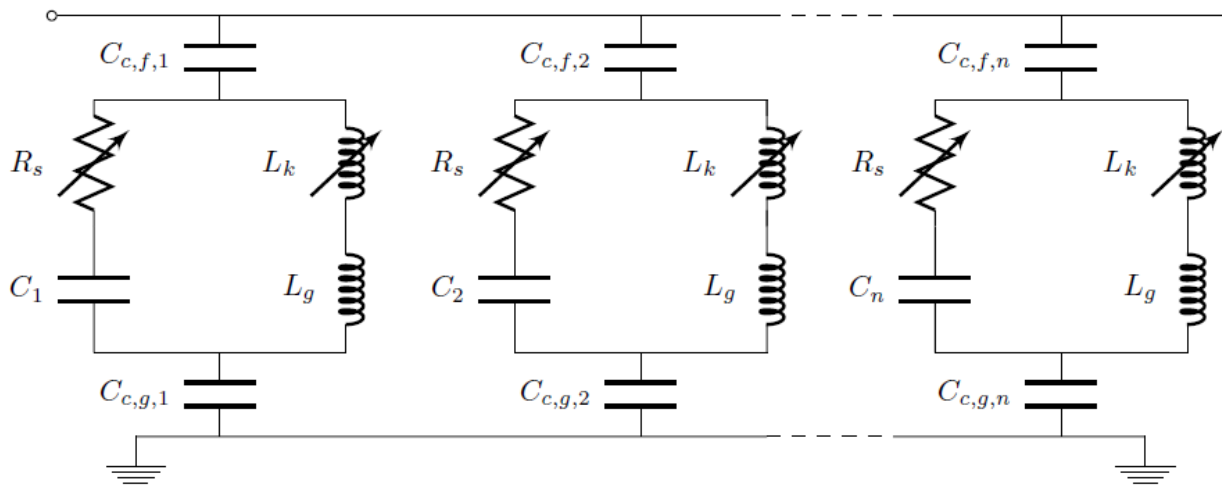
Front-Illumination



OLIMPO – KIDs



Front-Illumination

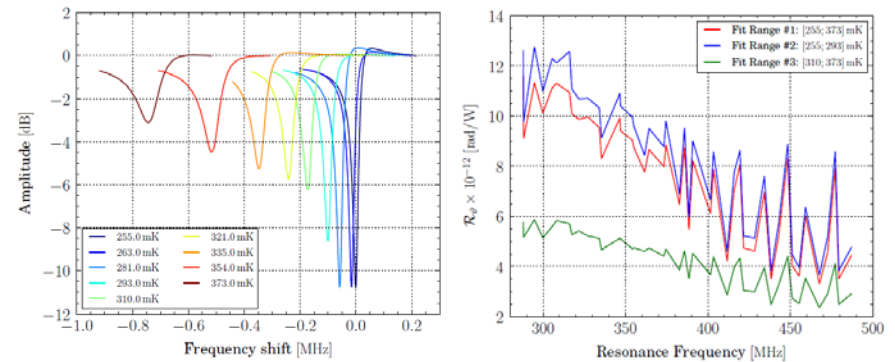
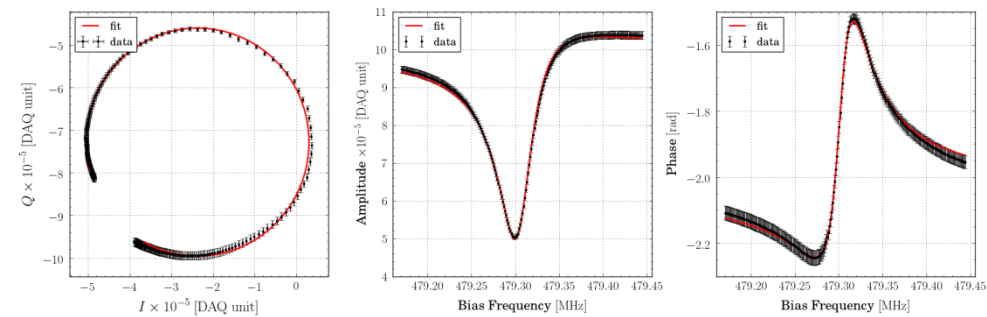
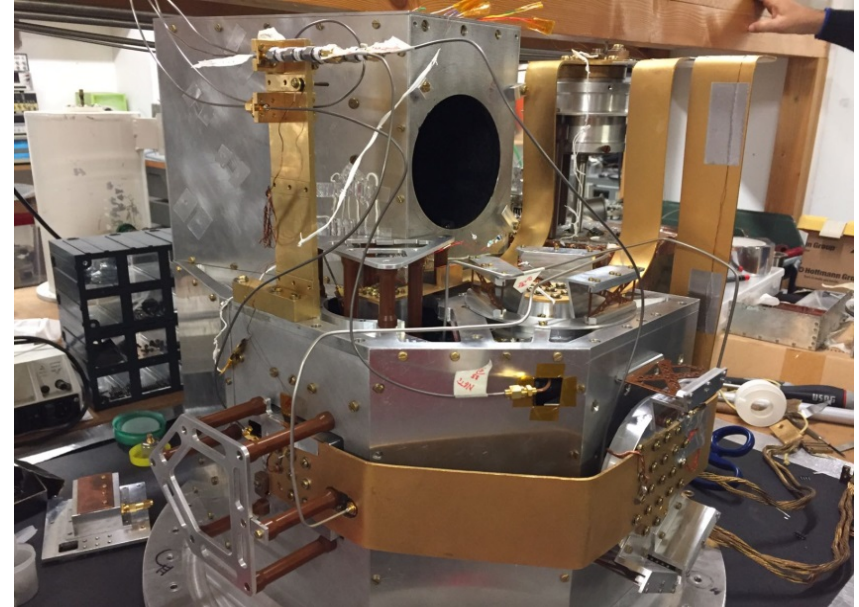
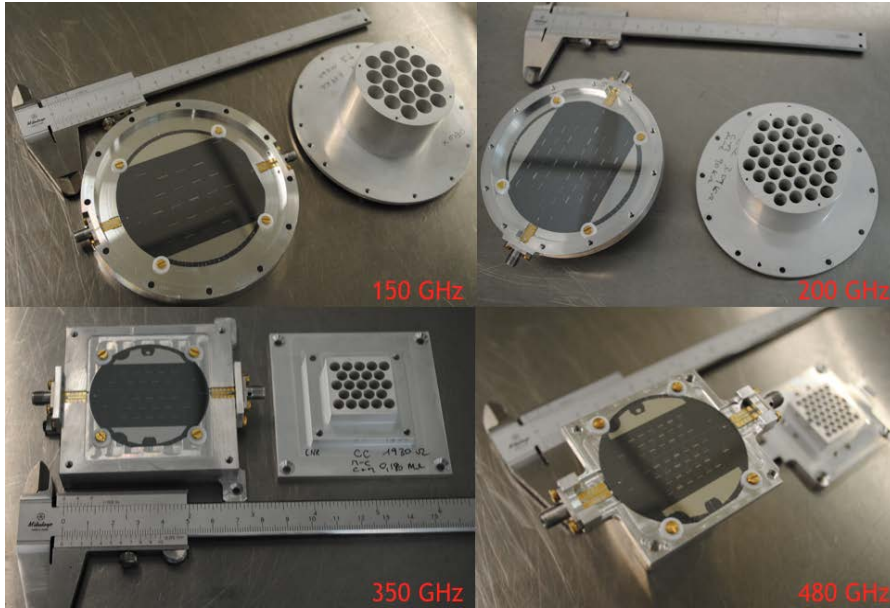


KID 1

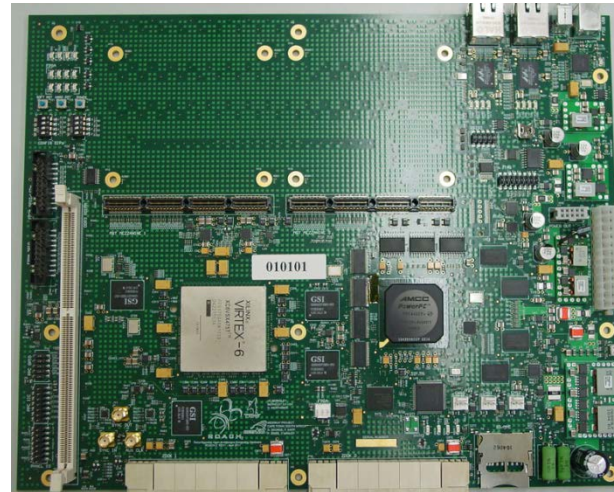
KID 2

KID n

OLIMPO – KIDs



OLIMPO – readout



ROACH-2 boards (2x) featuring:

- Virtex-6 SX475T FPGA
- PowerPC 440EPx stand-alone processor (control functions)

MUSIC DAC/ADC Mezzanine

VALON 5007 Oscillator as LO and MUSIC clock

ADL5385/87 boards for quadrature mod/demod

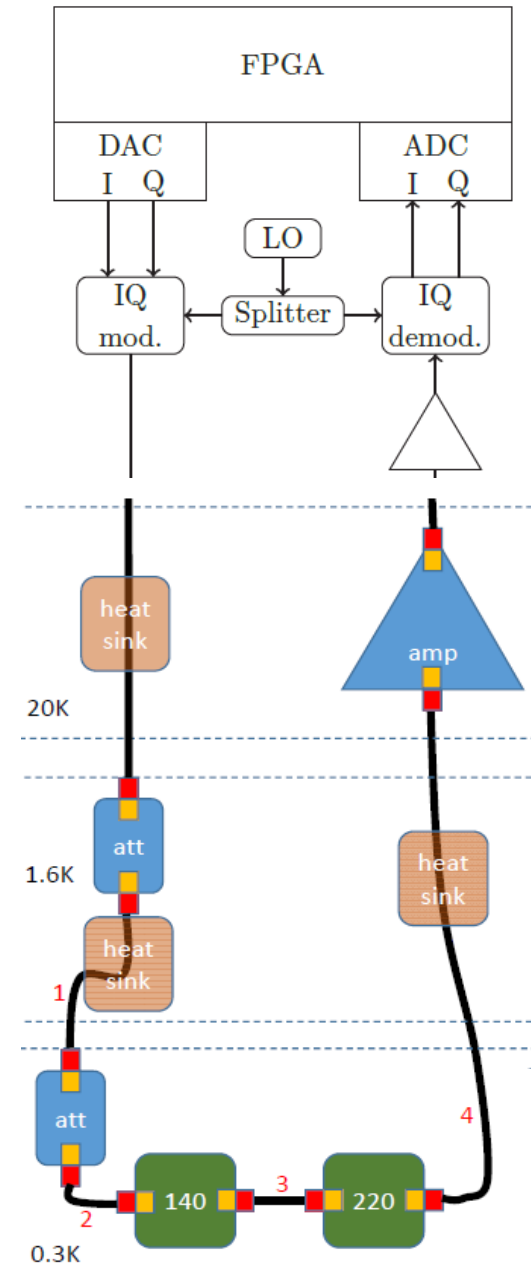
Filters, Bias Tees, Attenuators

Cryogenic LNAs developed by ASU

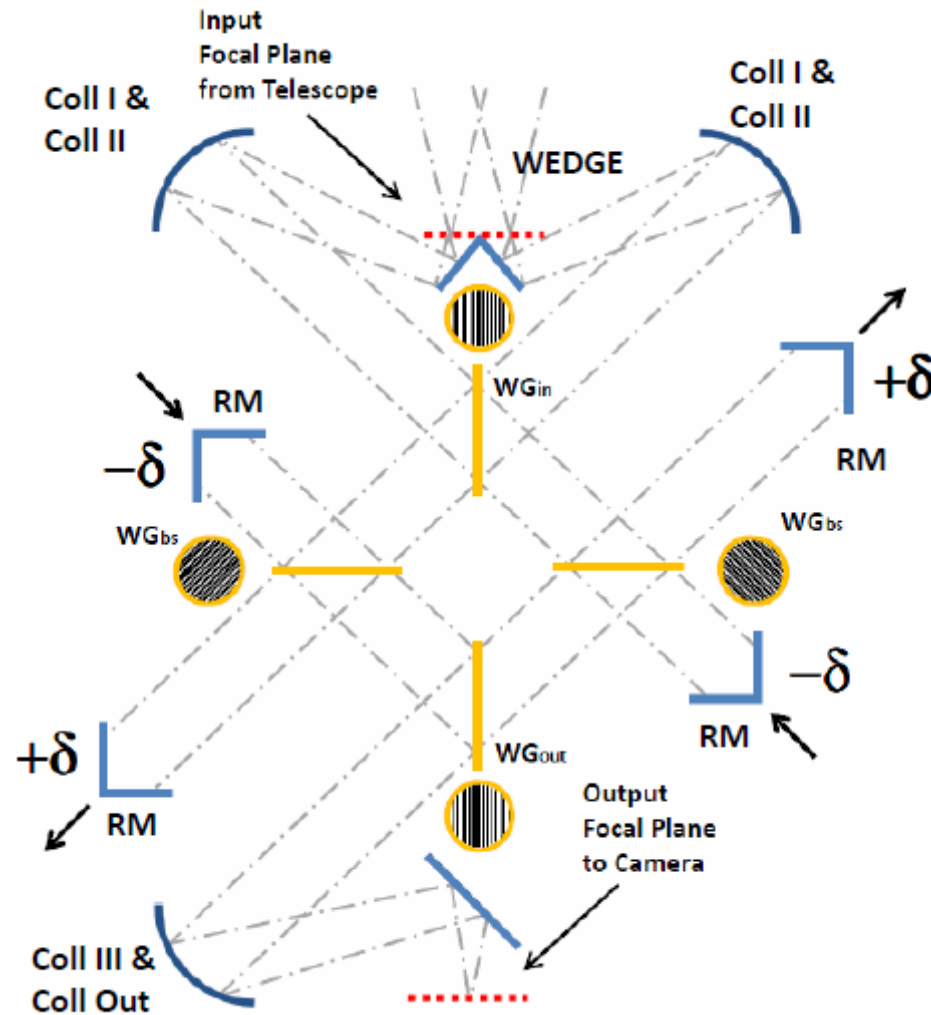
+Firmware provided by ASU

+Python code for interfacing and acquisition management

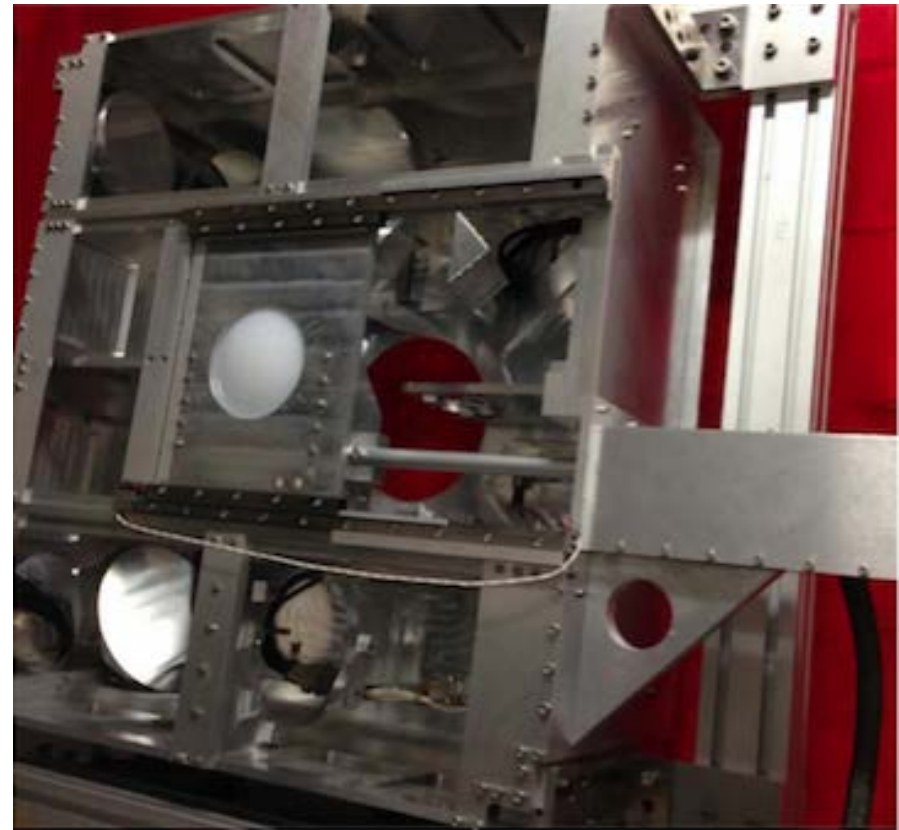
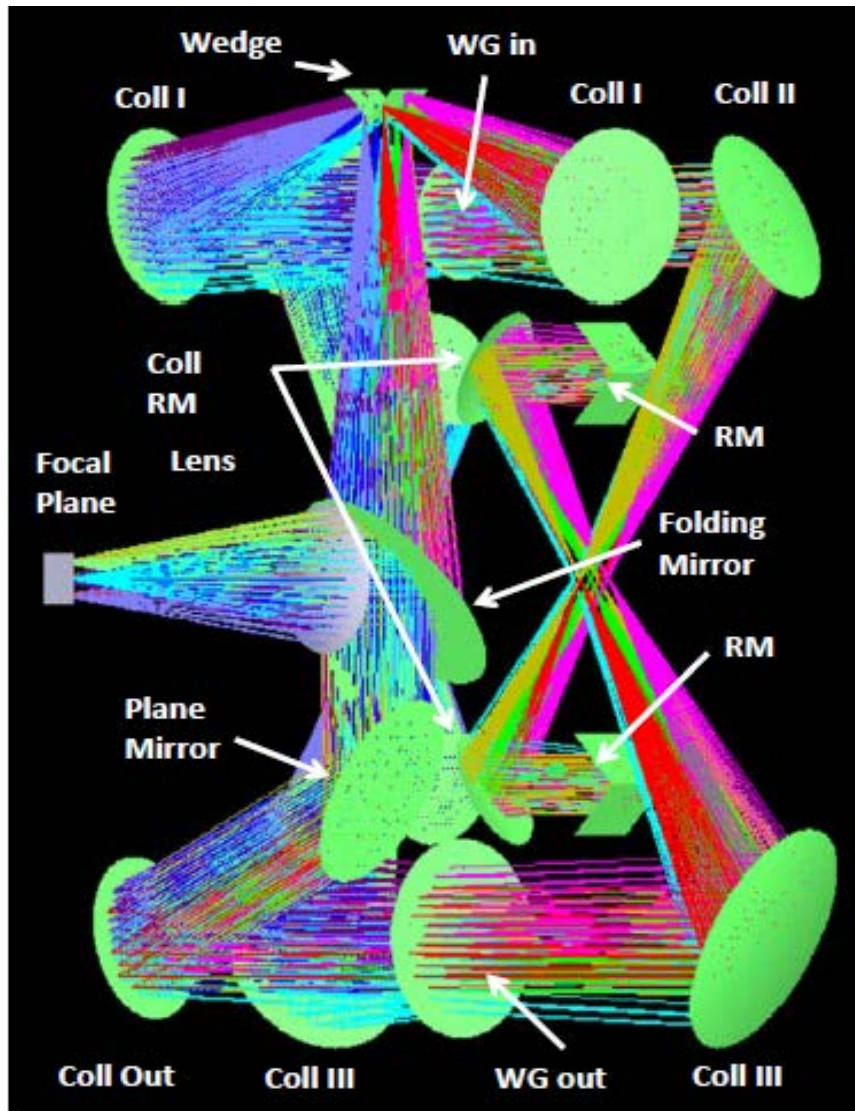
Readout scheme/hardware derived from the BLAST-TNG readout – Gordon et al., J. Astr. Instr., Volume 5, Issue 4, id. 1641003 (2016)



OLIMPO – Differential FTS



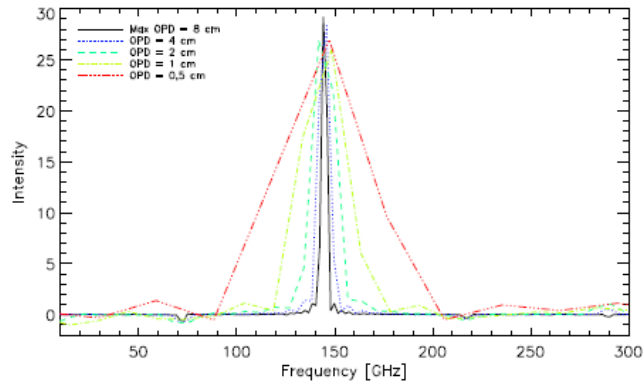
OLIMPO – Differential FTS



Schillaci et al., *Astronomy & Astrophysics*, Volume 565, id.A125 (2014)

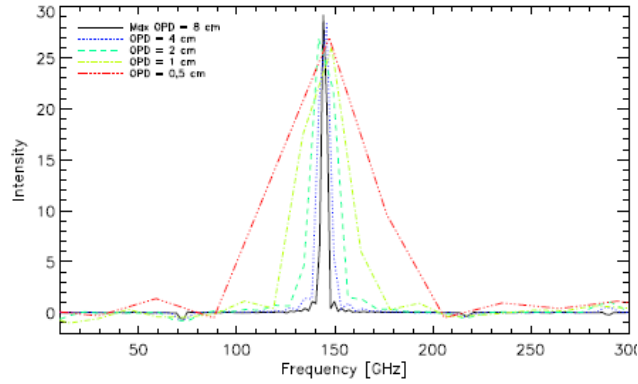
OLIMPO – DFTS characterization

Resolution

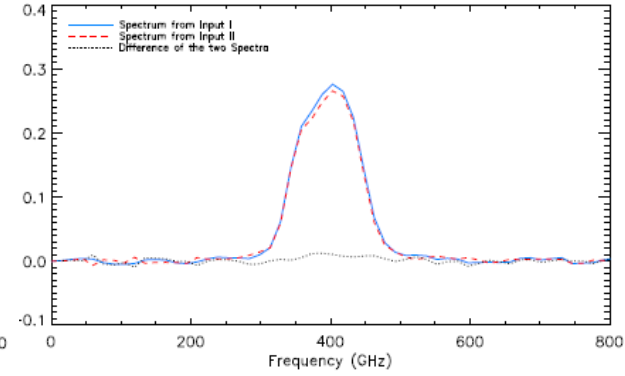
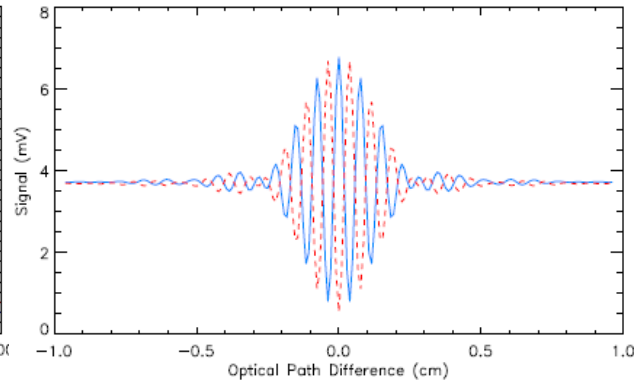


OLIMPO – DFTS characterization

Resolution

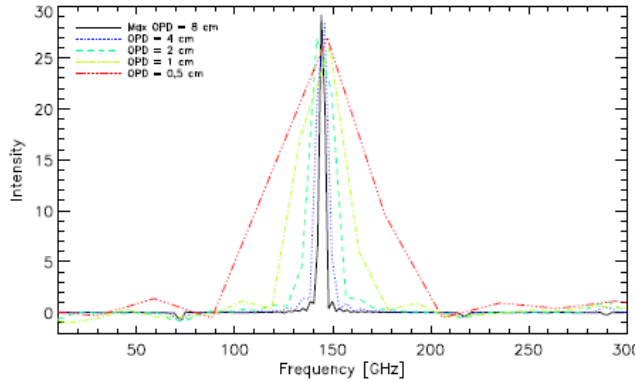


High freq efficiency and left/right FTS balance

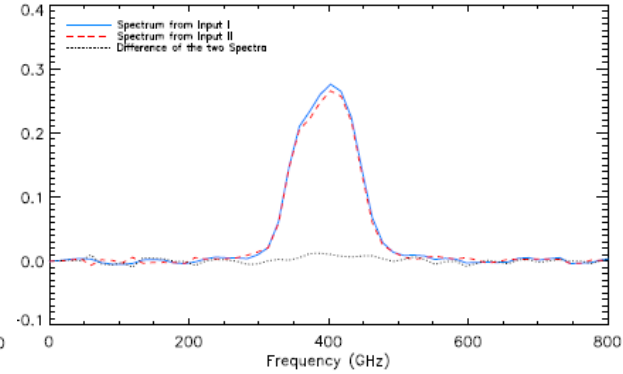
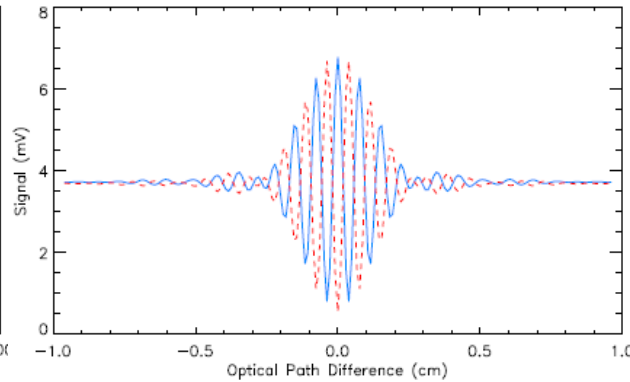


OLIMPO – DFTS characterization

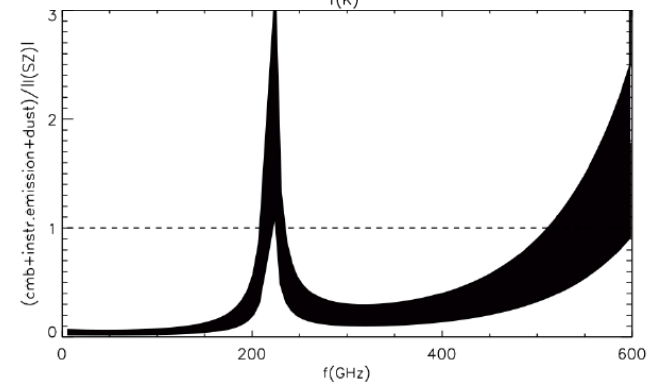
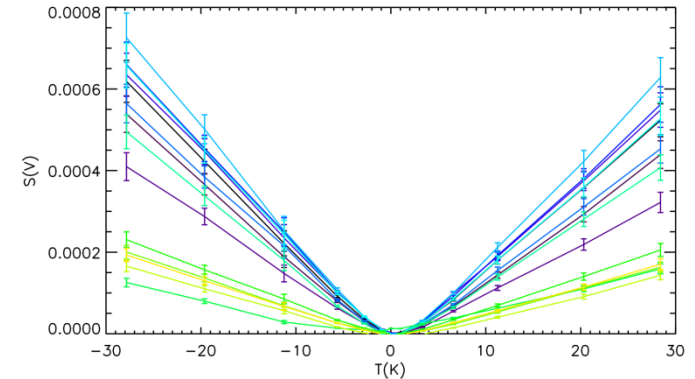
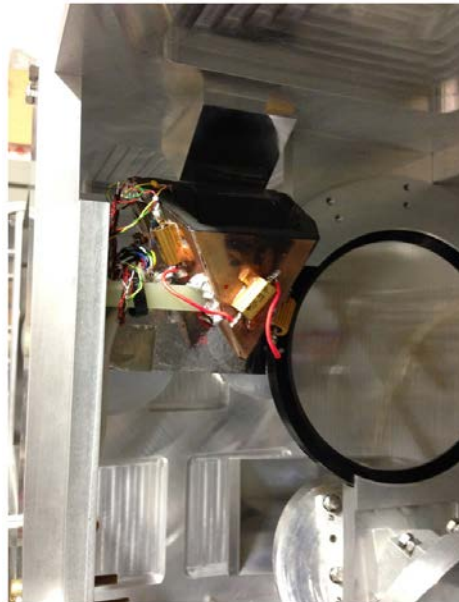
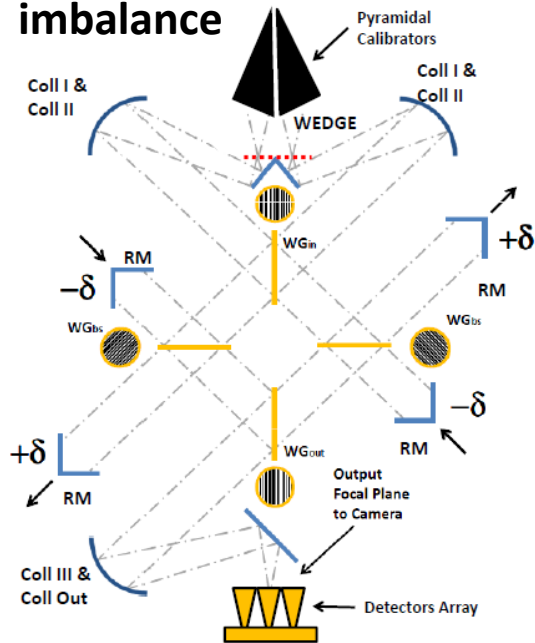
Resolution



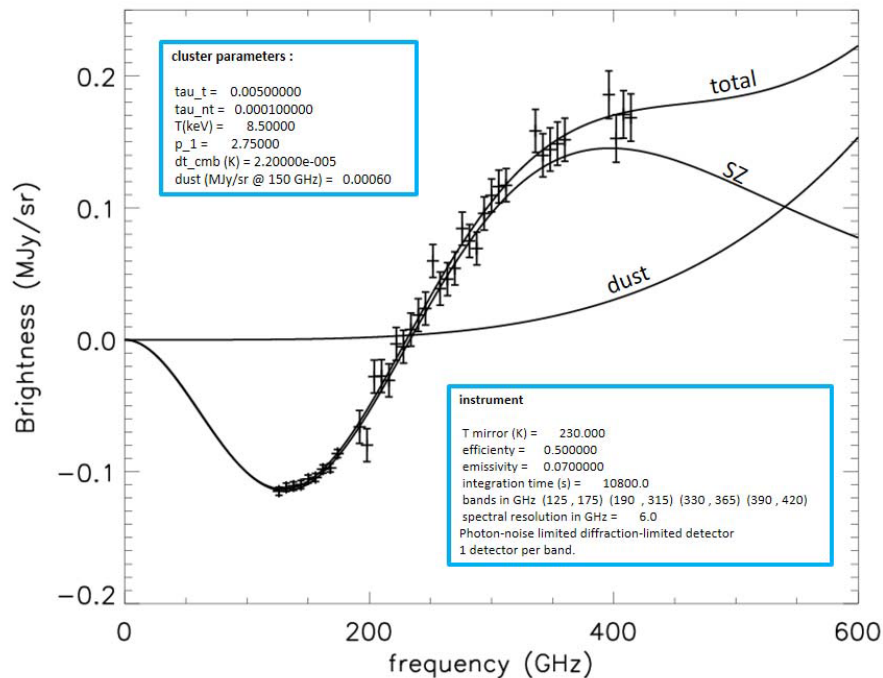
High freq efficiency and left/right FTS balance



Common mode rejection and thermal/optical imbalance



OLIMPO – end-to-end performance



DFTS resolution can be adjusted with almost no effort.

Noise/bin is proportional to the inverse of the spectral bin-width.

In the case of OLIMPO, with telescope and spectrometer at 250K, photon noise from optics emission is important.

- 1.8 GHz res: About 110 independent spectral bins
- 6 GHz res: About 34 independent spectral bins, within the same bands.

Observations from 10° to 60° elevation
40 targeted clusters S/N=10

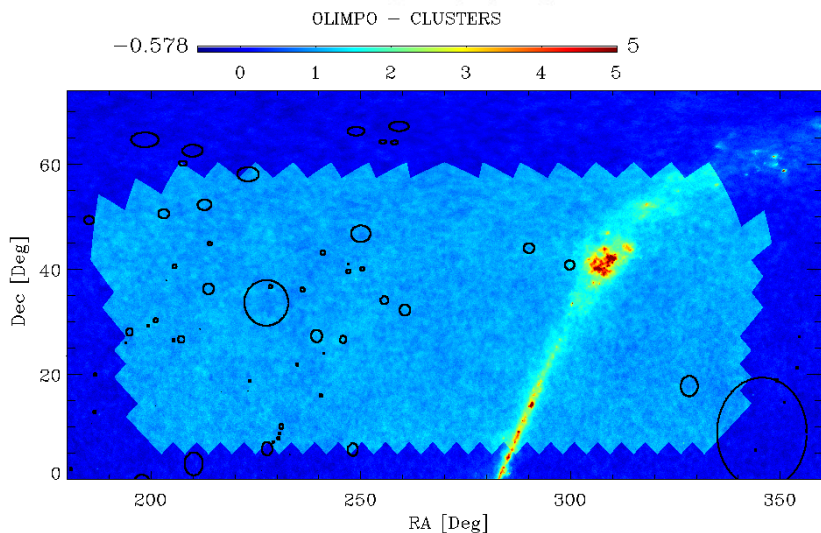
min=1h, max=5h

Single flight products:

34-frequency maps of selected sky regions (4 sq. deg. tiles, 2' FWHM res) on ~40 clusters and ~40 blank-sky regions.

Conversi et al., A&A 504 A7 (2010)

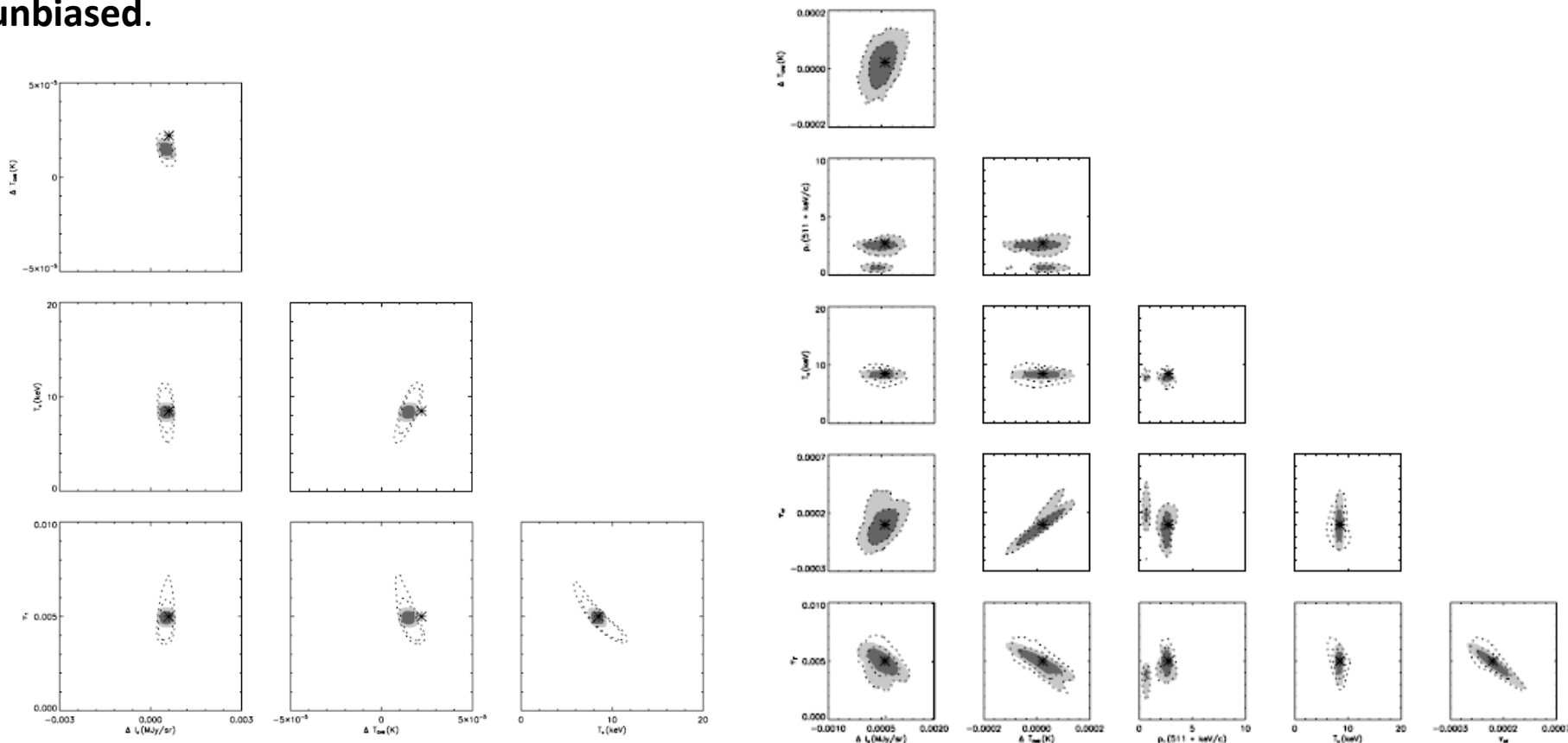
De Bernardis, LL, et al., A&A 538 A86 (2012)



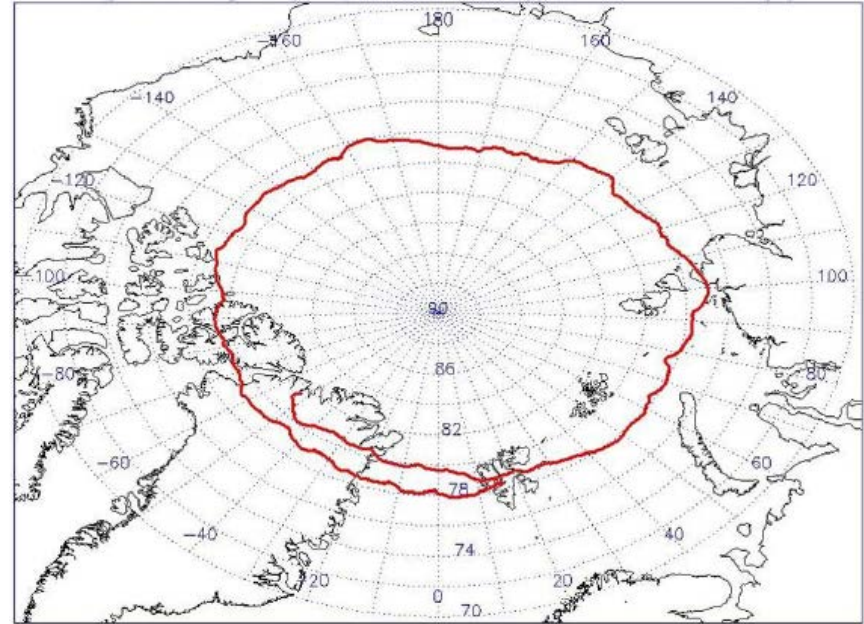
OLIMPO – end-to-end performance

Simulations of OLIMPO observations in DFTS configuration show that the spectroscopic configuration has superior performance in converging to the correct estimate of thermal optical depth and dust parameters, while the photometric configuration tends to converge to biased estimates of the parameters.

In particular the separation of thermal SZ and foreground dust emission is **effective** and **unbiased**.



OLIMPO – flight



The former version of OLIMPO (featuring past-gen TES detectors) was integrated in July 2014 for its first scientific flight from Svalbard Islands (78°N)

After on-the-field testing of all the subsystems (but NO launch due to adverse conditions), it has been funded for the upgrade to the KID configuration.

Launch was rescheduled to Summer 2018.



Concluding remarks

- SZ spectroscopy is both reliable and versatile in precision observations of galaxy clusters.
- The technology is mature and compatible with current and next-gen mm instrumentation.
- OLIMPO is not the only solution: the DFTS design has already been adapted and studied for both space and ground-based platforms (different spectral coverage, different limiting factors, but also different opportunities for making great science)
- Ground-based operation from cold and dry sites, in particular, could combine excellent spectral sensitivity with the advantage of a large aperture telescope (Antarctica?). Unfortunately, there are currently no plans to upgrade existing facilities to perform spectroscopy.
- Many adaptations already studied (APEX, SAGACE, MILLIMETRON...)

ありがとうございました！

